

REPORT NO.  
UC SESM 71-14

STRUCTURES AND MATERIALS RESEARCH  
DEPARTMENT OF CIVIL ENGINEERING

AD 731 719

# SOLVING THE GALVANIC CELL PROBLEM IN FERRO-CEMENT

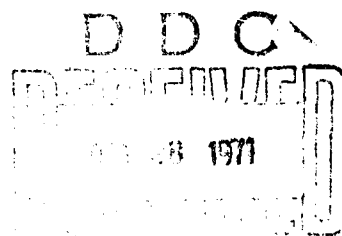
by

KENNETH A. CHRISTENSEN

and

ROBERT BRADY WILLIAMSON

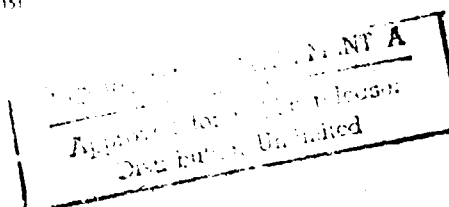
This research was sponsored by  
the Office of Naval Research under  
Contract N 00014-69-A-0200-1007.  
Project NR 032 522.  
This is TECHNICAL REPORT NO. 2



JULY 1971

STRUCTURAL ENGINEERING LABORATORY  
UNIVERSITY OF CALIFORNIA  
BERKELEY CALIFORNIA

Reproduced by  
NATIONAL TECHNICAL  
INFORMATION SERVICE  
Springfield, MA 01104



67

Structures and Materials Research  
Department of Civil Engineering

Report No. UCSESM 71-14

SOLVING THE GALVANIC CELL PROBLEM  
IN FERRO-CEMENT

by

Kenneth A. Christensen

and

Robert Brady Williamson

Details of illustrations in  
this document may be better  
studied on microfiche

This research was sponsored by the Office of Naval Research  
under Contract N 00014-69-A-0200-1007, Project NR 032 522.  
This is TECHNICAL REPORT NO. 2.

Reproduction is permitted  
for any purpose of the  
United States Government

Structural Engineering Laboratory  
University of California  
Berkeley, California

July 1971

Unclassified

## Security Classification

## DOCUMENT CONTROL DATA - R &amp; D

(Security classification of title, body of abstract and indexing annotation must be entered when the overall report is classified)

1. ORIGINATING ACTIVITY (Corporate author) Department of Civil Engineering University of California, Berkeley Berkeley, California 94720		2a. REPORT SECURITY CLASSIFICATION Unclassified	
		2b. GROUP none	
3. REPORT TITLE  THE GALVANIC CELL PROBLEM IN FERRO-CEMENT			
4. DESCRIPTIVE NOTES (Type of report and inclusive dates) Interim technical report			
5. AUTHOR(S) (First name, middle initial, last name)  Kenneth A. Christensen and Robert Brady Williamson			
6. REPORT DATE July 1971		7a. TOTAL NO. OF PAGES 56	7b. NO. OF REFS 16
8a. CONTRACT OR GRANT NO. N00014-69-A-0200-1007		9a. ORIGINATOR'S REPORT NUMBER(S)  Technical Report No. 2	
b. PROJECT NO. NR 032 522		9b. OTHER REPORT NO(S) (Any other numbers that may be assigned this report) UCSESM 71-14	
c.			
d.			
10. DISTRIBUTION STATEMENT  Reproduction in whole or in part is permitted for any purpose of the United States Government.			
11. SUPPLEMENTARY NOTES		12. SPONSORING MILITARY ACTIVITY  Office of Naval Research	
13. ABSTRACT  The nature and constitution of ferro-cement is reviewed with special reference to the structure of cement paste. The microstructure of low water-to-cement ratio pastes is presented in schematic illustrations to show that a thin paste layer can be used to protect steel reinforcing material from a marine environment. A galvanic cell between the plain steel reinforcing bar and the galvanized steel mesh ordinarily used in ferro-cement is identified. This galvanic cell gives off hydrogen gas at the plain steel reinforcing bar which leads to poor bonding. Possible solutions to this problem are presented and one, the use of chromium trioxide (CrO <sub>3</sub> ) in the mix water, is shown to solve the problem most effectively. This leads to improved mechanical properties as well as a sounder barrier to corrosion of the reinforcement.			

DD FORM 1473

Unclassified  
Security Classification

Unclassified

Security Classification

14	KEY WORDS	LINK A		LINK B		LINK C	
		ROLE	WT	ROLE	WT	ROLE	WT
	Ferro-cement						
	Galvanic Cell						
	Galvanized Reinforcing Steel						
	Chromium Trioxide						
	Passivation						

Unclassified

Security Classification

### ABSTRACT

The nature and constitution of ferro-cement is reviewed with special reference to the structure of cement paste. The microstructure of low water-to-cement ratio pastes is presented in schematic illustrations to show that a thin paste layer can be used to protect steel reinforcing material from a marine environment. A galvanic cell between the plain steel reinforcing bar and the galvanized steel mesh ordinarily used in ferro-cement is identified. This galvanic cell gives off hydrogen gas at the plain steel reinforcing bar which leads to poor bonding. Possible solutions to this problem are presented and one, the use of chromium trioxide ( $\text{CrO}_3$ ) in the mix water, is shown to solve the problem most effectively. This leads to improved mechanical properties as well as a sounder barrier to corrosion of the reinforcement.

TABLE OF CONTENTS

	<u>Page</u>
1. Introduction	
1.0 General . . . . .	1
1.1 Forward to the Report . . . . .	1
2. Nature and Constitution of Ferro-Cement	
2.0 Definition and History . . . . .	2
2.1 Constitution of Ferro-Cement . . . . .	4
2.2 Factors Leading to the Galvanic Cell Problem . . . . .	15
3. Galvanic Cell Problem	
3.0 The Problem . . . . .	18
3.1 Recognition of the Problem . . . . .	21
3.2 Possible Solutions of the Problem . . . . .	22
4. Solution to Galvanic Cell Problem - Experimental Results	
4.0 Experimental Methods and Materials . . . . .	25
4.1 Experimental Results . . . . .	33
4.2 Microscopic Observations . . . . .	44
4.3 Conclusions and Recommendations . . . . .	54

# LIST OF FIGURES

<u>Figure</u>	<u>Page</u>
2.1 Graphical representation of relative volume of hydration products . . . . .	8
2.2 Inner and outer hydration products . . . . .	9
2.3 Schematic hydration of cement paste (W/C~.5) . . . . .	10
2.4 Schematic hydration of cement paste of low water-to-cement ratio . . . . .	11
3.1 The nature of the zinc-iron galvanic cell . . . . .	18
3.2 Galvanic cell between galvanized mesh and plain steel reinforcing bar . . . . .	19
4.1 Cross section, $\frac{3}{4}$ -in ferro-cement test specimen . . . . .	31
4.2 Cross section, $\frac{1}{2}$ -in ferro-cement test specimen . . . . .	31
4.3 Ferro-cement panels with $\text{CrO}_3$ one hour after casting . . . . .	34
4.4 Ferro-cement panels without $\text{CrO}_3$ showing bubbles frozen on top surface . . . . .	37
4.5 Surface of mortar in contact with the reinforcement steel - both with and without $\text{CrO}_3$ . . . . .	39
4.6 Flexure test experiment of ferro-cement . . . . .	40
4.7 Load deflection curves of flexure tests showing increased strengths of $\text{CrO}_3$ treated specimens . . . . .	42
4.8 Mortar/reinforcing bar surface with all galvanized, all black steel, and epoxy coated steel . . . . .	45

<u>Figure</u>	<u>Page</u>
4.9    Rough mortar/steel surface without $\text{CrO}_3$ shown by scanning electron micrographs . . . . .	47
4.10   Higher magnification views of an area marked in Figure 4.9 . . . . .	48
4.11   Smooth mortar/steel surface with $\text{CrO}_3$ shown by scanning electron micrographs . . . . .	50
4.12   A sequence of higher magnification micrographs of mortar surface with $\text{CrO}_3$ of an area marked in Figure 4.11 . . . . .	52



### ACKNOWLEDGEMENTS

We would like to express our gratitude to the many colleagues who assisted us in this study. We wish to convey special thanks to Professor Jerome Raphael who gave us such strong support and encouragement. We would like to express our deepest appreciation to Tim Snyder, George Hayler, and all the others who helped in special ways to make this study possible. Finally, we would like to thank Professors Boris Bresler and Israel Cornet who had already solved our problem before we found it, and then shared their experiences to help us optimize the treatment.

## 1. INTRODUCTION

### 1.0 General

The practical application of laboratory research projects is often very difficult to accomplish. All too often the research engineer or scientist is not aware of the practical problems, and thus even if he learns the answer to a particular question, he does not recognize it since he did not know the question in the first place. On the other hand a problem develops in the practice of engineering and a solution is found empirically without the deeper understanding of the research-oriented worker. This report is one in a series on the applied science of cementitious materials.

### 1.1 Forward to the Report

This is the second technical report of a research project on "The Relationship between Microstructure and Mechanical Properties of Cementitious Materials" which is being performed in the Division of Structural Engineering and Structural Mechanics, Department of Civil Engineering, University of California at Berkeley.

This report is the first of several reports on specific aspects of "ferro-cement," Ferro-cement is a combination of reinforcing wire and cement mortar that can be used in thin shell construction. It is highly adaptable for boat hulls and other marine applications, and it is in this application that it has gained its widest acceptance.

## 2. NATURE AND CONSTITUTION OF FERRO-CEMENT

### 2.0 Definition and History

A working definition of ferro-cement is that it is a thin shell of highly reinforced Portland cement mortar. Generally, the shells are in the range of  $\frac{1}{2}$ -in to  $1\frac{1}{2}$ -in thickness, and the reinforcement is in the form of as many layers of steel mesh as possible for a given thickness with or without steel reinforcing bars sandwiched midway between the layers of mesh. The resulting shell or panel is impregnated with a very rich portland cement mortar. It might be thought that this is simply the well-known engineering material reinforced concrete. This is not the case. It has been thoroughly demonstrated that ferro-cement behaves in a manner so different from concrete reinforced with steel that it has to be considered as an entirely different material, (1,2). Because the mesh is so finely and evenly distributed and subdivided throughout the entire cross section of the shell, there is a synergistic effect. Shah (1) observed that the fracture strength of ferro-cement primarily is dependent on the load carrying capacity of the mesh reinforcement. Shah notes that the modulus of elasticity of ferro-cement can be estimated from the wire mesh alone, however for strain and cracking he finds a significant interaction between matrix and reinforcement. Shah found the specific surface of reinforcement, thus the total bonding area between mortar and steel, to be the most sensitive parameter as far as strain and cracking were concerned. The specific surface of reinforcement is considerably higher for ferro-cement than for reinforced concrete, and this is

one of the factors that distinguishes one from the other.

Ferro-cement is used in thin wall (shell) applications where strength and rigidity are developed through form or shape. It has the distinct advantage of being moldable and of one piece construction. Other major advantages are its low cost and its nonflammable and low corrosive characteristics. The use in thin shells is possible because ferro-cement has relatively high tensile strength and essentially a homogeneous, crack-free behavior.

The colorful history of ferro-cement has been reviewed in several places (3,4) and it has many interesting sagas. Although its history goes back over 50 years, there is general agreement that the first serious research and development efforts were undertaken by the Italian Naval Administration in the spring of 1943. Several motor-driven cargo vessels of 400 tons capacity were started by the firm of Nervi and Bartoli. Their construction was interrupted by the war, but there was renewed interest following the war. Some of the original vessels were finished, and several new ones were constructed. The operational experience of these vessels over a period of 10-20 years was judged highly successful.

Following his original investigations for the Italian Navy, Pier Luigi Nervi successfully used ferro-cement for buildings and other civil engineering structures (5). They have become landmarks of modern design. There are many potential uses of ferro-cement that could be developed in the future as more is learned about the material.

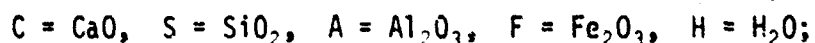
The durability of ferro-cement is particularly well-illustrated in the following passage from the Russian engineer, I. Ya Glan:

"The first reinforced concrete (read ferro-cement) yacht 'Opyt' (Experience) in late autumn 1957 was torn from anchor during a severe storm and was thrown onto the rocks on the opposite shore. We were unable to remove the yacht because of the ice jam which had started. The entire autumn, the hull of the yacht was on the rocks, and during the winter it froze into the ice. In the spring, at first glance the hull of the yacht had a sad appearance. The sides were crumpled, but nevertheless the reinforced gratings proved to be undamaged. All that was required was the work of four men, a bag of cement and several buckets of river sand in order for the yacht hull to be repaired in one day" (ref 4, p 6).

## 2.1. Constitution of Ferro-Cement

The combination in ferro-cement of steel mesh and portland cement mortar means that the design engineer must know about each material separately and their interactions. The solidification or hardening of portland cement is the basic reaction in the fabrication of ferro-cement. The solidification of portland cement has been extensively discussed in the first technical report on this project (6), but it will be reviewed briefly here.

The reaction of portland cement and water is the basic chemical reaction associated with the hardening of cement paste. The subsequent carbonation of the hydration products is not necessary for them to gain strength, and this often is associated with the deterioration of cement. Anhydrous portland cement contains four principal compounds: tricalcium silicate,  $\beta$ -dicalcium silicate, tricalcium aluminate, and a solid solution series which until recently was generally believed to have the fixed composition of tetracalcium alumino ferrite. The composition of cement compounds are often represented as the sum of oxides, the formulae of which are abbreviated:



thus, for example, tricalcium silicate,  $\text{Ca}_3\text{SiO}_5$  is represented by  $3\text{CaO}\cdot\text{SiO}_2$  and shortened to just  $\text{C}_3\text{S}$ . This system is used in cement chemistry interchangeably with ordinary chemical notation. The typical composition of the four standard types of portland cement used in the United States are given in Table 2.1 with the abbreviated forms shown in addition to the chemical names. Small amounts of  $\text{MgO}$ ,  $\text{CaO}$  and alkali sulphates also occur in many cements. The types of cements shown in Table 2.1 are characterized by particular properties as noted. Type II is usually recommended for ferro-cement since it has high resistance to attack by sea water. This resistance to sea water

Table 2.1. Proportions of Major Compounds in Four Basic Types of Portland Cement Made in the U.S.A.

	I General Use	II Moderate Heat of Hardening	III High Early Strength	IV Low Heat of Hardening
TRICALCIUM SILICATE $\text{C}_3\text{S}$	53	47	58	26
B-DICALCIUM SILICATE $\text{B-C}_2\text{S}$	24	32	16	54
TRICALCIUM ALUMINATE $\text{C}_3\text{A}$	8	3	8	2
CALCIUM ALUMINATE FERRITE SOLID SOLUTION Between $\text{C}_2\text{F}$ and $\text{C}_6\text{A}_2\text{F}$	8	12	8	12
Total	93	94	90	94

These are average percentages obtained by X-ray diffraction analysis of several cements. The remaining 6-7% consists of 2-3%  $\text{CaSO}_4$ , 0.2-0.8% free  $\text{CaO}$ , and trace amounts of moisture, insoluble residue and alkali oxides combined in various ways (6).

attack is usually associated with lower concentrations of tricalcium aluminate. There is also a Type V cement which has special controls to assure even better sea water resistance. The fractions shown in Table 2.1 are typical values determined by X-ray diffraction and do not represent the legal limits for each type of cement.

Each of the phases of portland cement react with water to give solid products that form the structure of portland cement paste. These reactions are shown in Table 2.2. Note that both tricalcium silicate and  $\beta$ -dicalcium silicate yield the same reaction products: a calcium silicate hydrate (C-S-H) and calcium hydroxide. The C-S-H material

Table 2.2. Principal Reactions of Portland Cement with Water

2(3CaO·SiO <sub>2</sub> ) (TRICALCIUM SILICATE)	+ 5.5H <sub>2</sub> O =	3CaO·2SiO <sub>2</sub> ·2.5H <sub>2</sub> O + 3Ca(OH) <sub>2</sub> (CALCIUM SILICATE HYDRATE) (PORTLANDITE)
2(2CaO·SiO <sub>2</sub> ) (DICALCIUM SILICATE)	+ 3.5H <sub>2</sub> O =	3CaO·2SiO <sub>2</sub> ·2.5H <sub>2</sub> O + Ca(OH) <sub>2</sub> (CALCIUM SILICATE HYDRATE) (PORTLANDITE)
4CaO·Al <sub>2</sub> O <sub>3</sub> ·Fe <sub>2</sub> O <sub>3</sub> + 10H <sub>2</sub> O + 2Ca(OH) <sub>2</sub> ("TETRACALCIUM ALUMINOFERROTE")		= 6CaO·Al <sub>2</sub> O <sub>3</sub> ·Fe <sub>2</sub> O <sub>3</sub> ·12H <sub>2</sub> O (CALCIUM ALUMINOFERRITE HYDRATE)
3CaO·Al <sub>2</sub> O <sub>3</sub> (TRICALCIUM ALUMINATE)	+ 12H <sub>2</sub> O + Ca(OH) <sub>2</sub>	= 4CaO·Al <sub>2</sub> O <sub>3</sub> ·13H <sub>2</sub> O (TETRACALCIUM ALUMINATE HYDRATE)
3CaO·Al <sub>2</sub> O <sub>3</sub>	+ 10H <sub>2</sub> O + CaSO <sub>4</sub> ·2H <sub>2</sub> O (GYPSUM)	= 3CaO·Al <sub>2</sub> O <sub>3</sub> ·CaSO <sub>4</sub> ·12H <sub>2</sub> O (CALCIUM MONOSULFO- ALUMINATE)

has drawn particular attention over the past twenty years, and its nature and properties are the subject of considerable discussion in the literature (6). The calcium hydroxide  $\text{Ca(OH)}_2$  constitutes an important constituent that has not received as much attention as the C-S-H. The calcium hydroxide is also known by its mineralogical name, portlandite, and this will be used in general.

The reactions of tricalcium aluminate and the iron bearing solid solution (labeled  $\text{C}_4\text{AF}$ ) are shown in Table 2.2, but for the most part these reactions do not greatly affect the properties of the hardened cement. Two reactions are shown in Table 2.2 for tricalcium aluminate, one with and one without gypsum,  $\text{CaSO}_4 \cdot 2\text{H}_2\text{O}$ . The gypsum is added to most portland cement as it is ground, a process called intergrinding, in order to prevent a premature setting of the paste.

In its simplest terms, the hydration of cement is a reaction in which a solid of low solubility reacts with water to form solid products of even lower solubility. The chemical reactions shown in Table 2.2 can be thought of in this simplified framework. A graphical representation shown in Figure 2.1 can be used to describe the sequence of events as the cement minerals react with water. This reaction produced the continuous solid matrix in the space that was originally occupied by discrete particles dispersed in the water. In Figure 2.1 the relative volume of water and cement are represented by a bar graph labeled "Fresh Paste" for the case of 0.5 water-to-cement ratio. The specific gravity of the cement has been taken at 3.15, and thus there is 1.55 cubic centimeters of water for one cubic centimeter of cement. The hydration reaction is then represented at 33%, 67%, and 100%



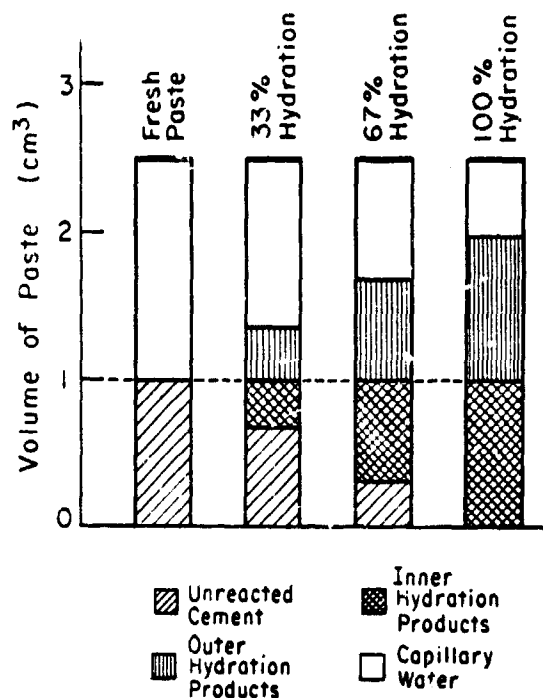


Figure 2.1. Graphical representation of the relative volumes of hydration products of portland cement at three stages of hydration: 33%, 67%, and 100% completion. The initial water-to-cement ratio is 0.5, and one unit volume of cement is shown to produce two unit volumes of hydration products.

completion on the basis that one half unit of cement yields one unit volume of hydration products. The nomenclature of inner and outer hydration products has been introduced into Figure 2.1 in order to discriminate between the products laid down within the boundaries of the original cement grains and the products laid down in the originally water-filled space.

The spatial relationship of the hydration products with respect to the original cement grain can be determined by microscopic investigation. The partial hydration of one grain of cement is schematically represented in Figure 2.2. There are many details in this process that

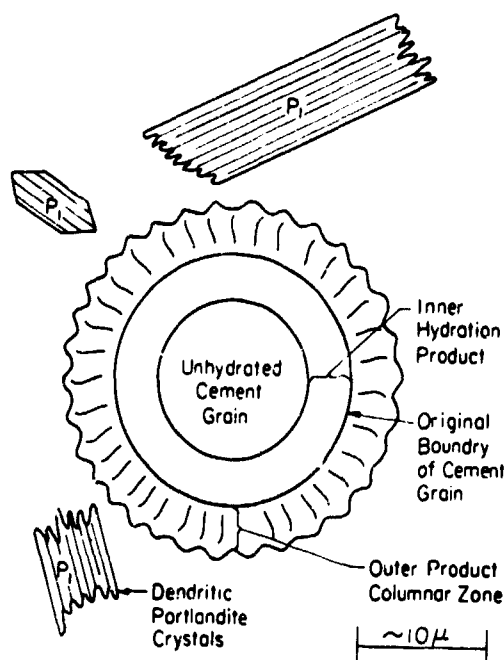
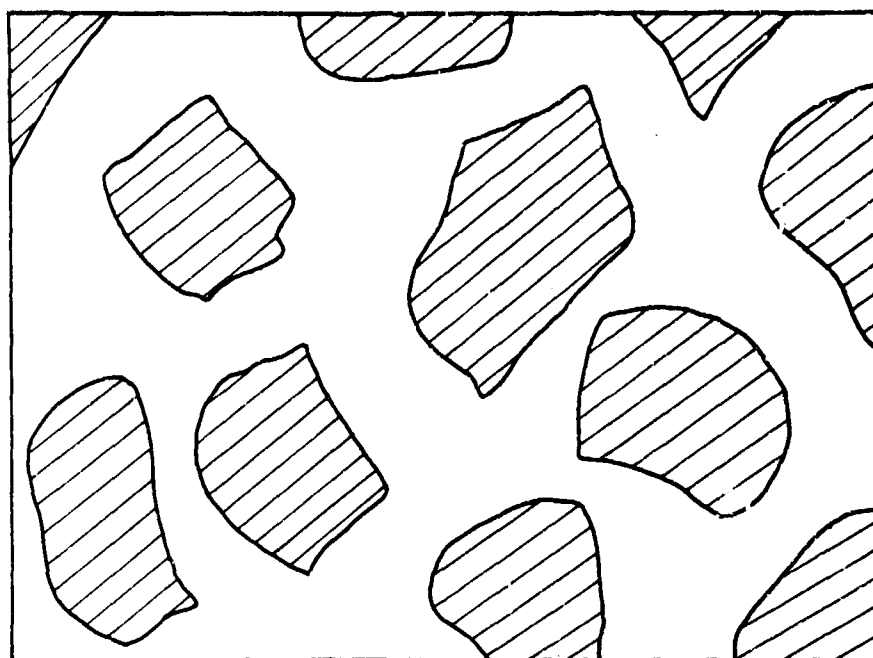


Figure 2.2. The hydration products formed inside and outside the cement grain are schematically represented. The multiple nature of the cement grain is neglected and is assumed to be a single phase that shows two types of hydration products.

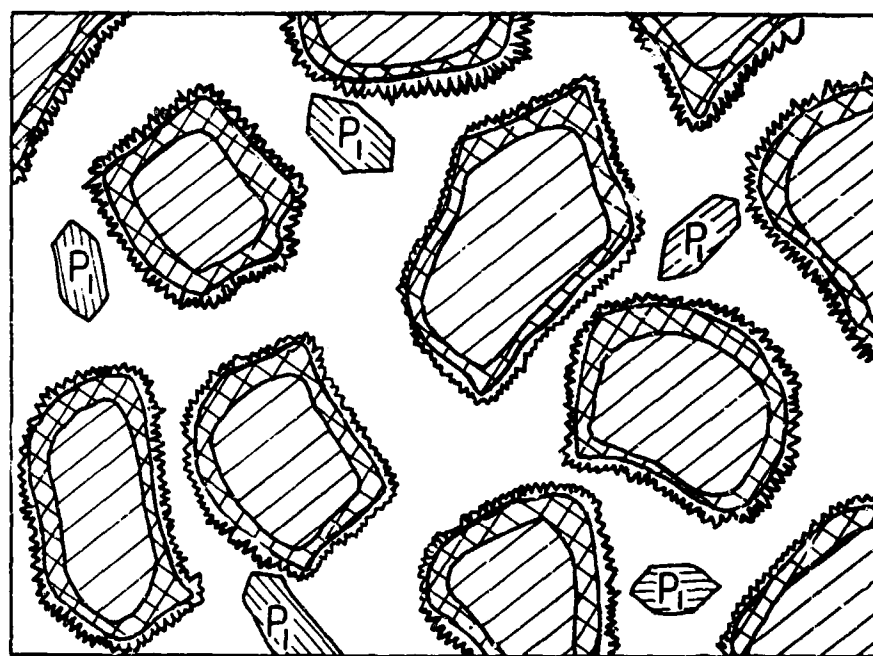
are not yet understood (6), but there is sufficient information available to allow a consistent mental picture to be constructed. This is one of the principal objectives of Williamson's descriptions of the solidification of portland cement.

The hydration of a number of cement grains is schematically represented in Figure 2.3 at different degrees of hydration. The fresh paste (i.e., the initial combination of water and cement grains) is drawn to approximately represent the 0.5 water-to-cement ratio shown in Figure 2.1. In this case there are not sufficient hydration products to fill the originally water-filled space and a capillary porosity remains in the final microstructure. The measure of this






FRESH PASTE

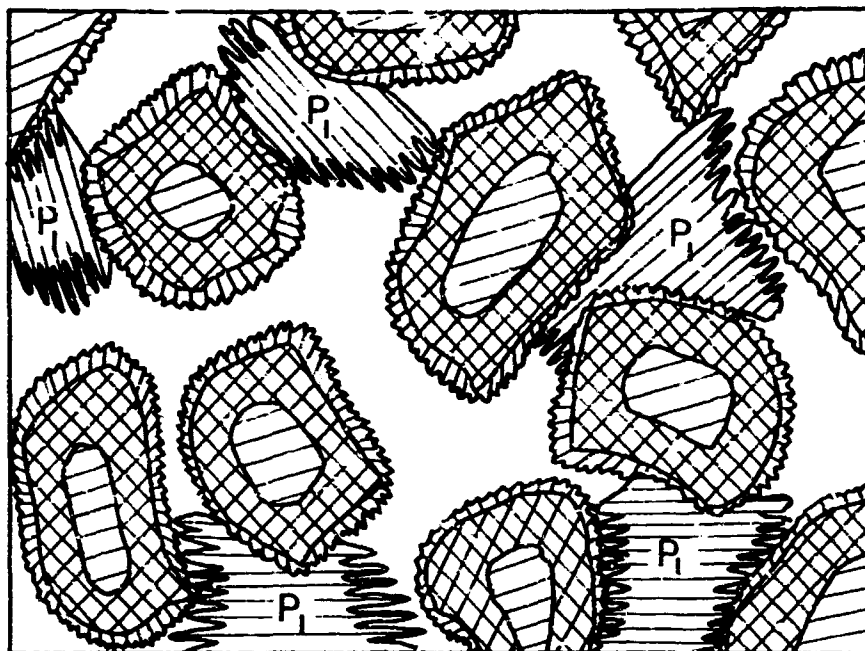
(a)



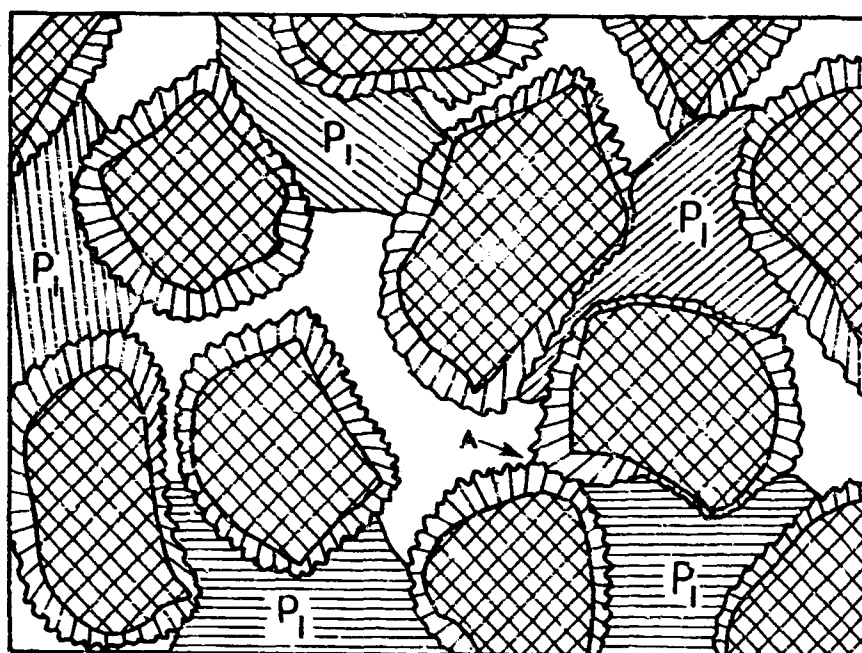
33% HYDRATED

(b)

Figure 2.3. A schematic representation of the hydration of cement based on the relative volumes shown in Figure 2.1. The multiphase nature of the cement grains has been neglected so this is like the hydration of tricalcium silicate alone. (a) Fresh paste of water-to-cement ratio of 0.5 is shown with unhydrated cement represented by  and the originally water-filled space clear. (b) After 33% hydration the inner hydration products are represented by  and the outer products by . The primary portlandite is labeled  $P_1$  and the columnar zone is shown around each grain.

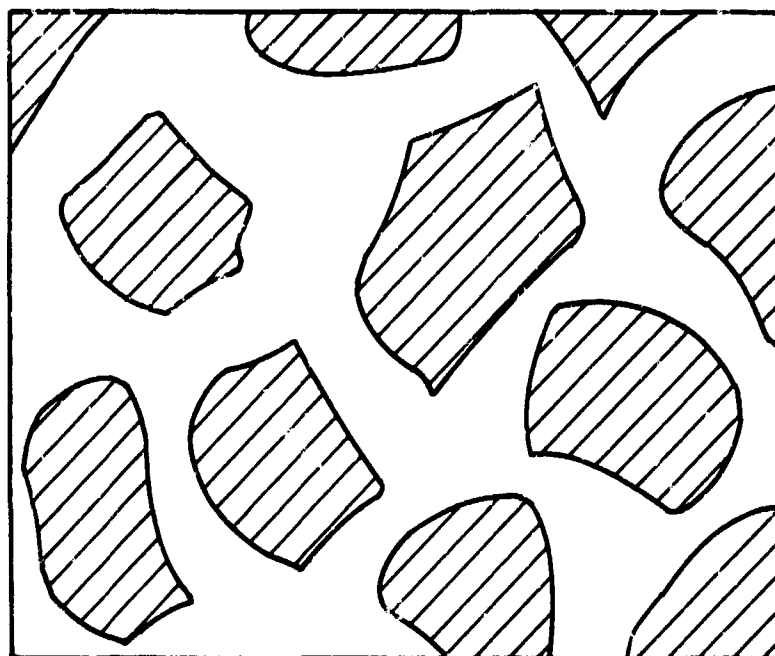


67 % HYDRATED (c)

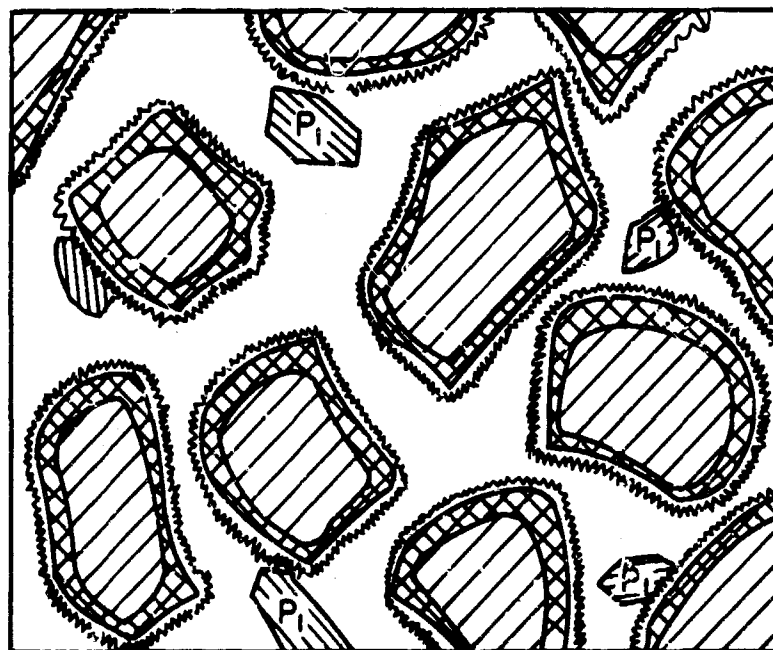


100 % HYDRATED (d)



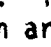
Figure 2.3. (Continued from opposite page)... (c) After 67% hydration the unhydrated cores are clearly surrounded by thick "rims" of inner hydration products and the columnar zone of outer products is growing on the outer surface of each grain. The primary portlandite,  $P_1$ , is shown with the dendritic morphology reported in the optical study of Berger and McGregor (6). (d) At 100% hydration the unhydrated cement has been consumed but the shape of the original cement grains can be distinguished if the inner product differs from the columnar zone of outer products. The intergrowth of the columnar zones from two different grains is only shown at one place, marked A, but this would be more common at lower water-to-cement ratios.

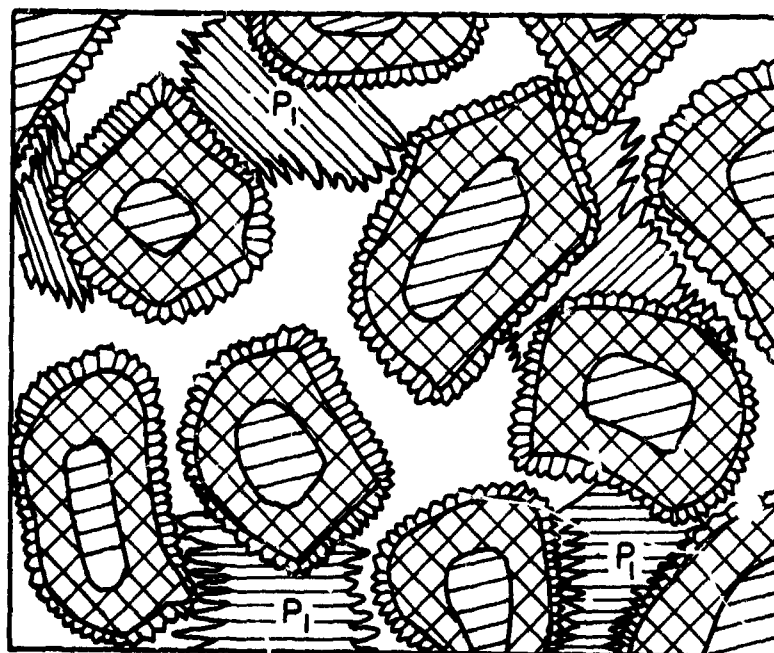


FRESH PASTE (a)

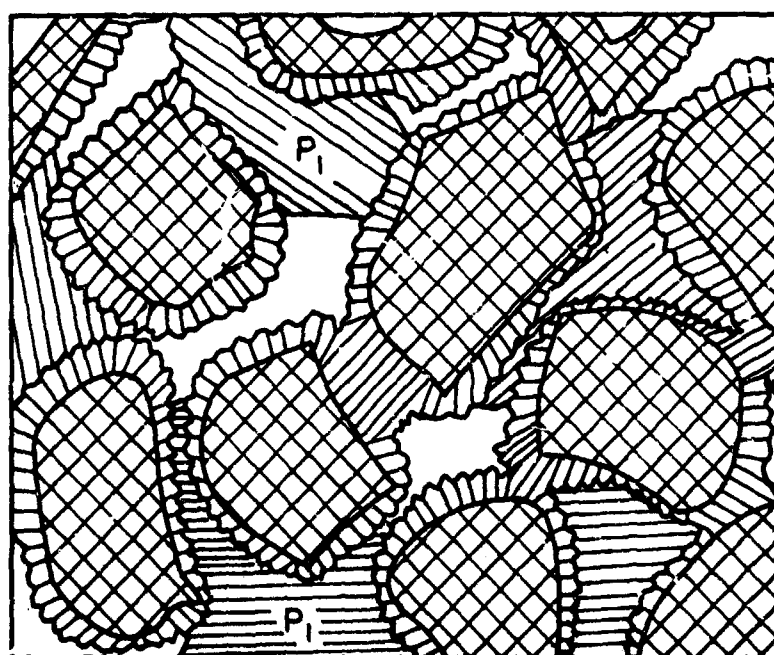


33% HYDRATED (b)

Figure 2.4. A schematic representation of the hydration of cement exactly the same as the previous figure except that the grains of cement have been moved closer together in order to represent a lower water-to-cement ratio (approximately 0.3). (a) Fresh paste is shown with unhydrated cement represented by  and the originally water-filled space clear. (b) After 33% hydration the inner hydration products are represented by  and the outer products by . The primary portlandite is labeled  $P_1$  and the columnar zone is shown around each grain.



67% HYDRATED (c)



100% HYDRATED (d)

Figure 2.4. (continued from opposite page)... (c) After 67% hydration the unhydrated cores are clearly surrounded by thick "rims" of inner hydration products and the columnar zone of the outer products is growing on the outer surface of each grain just as in the previous figure. (d) At 100% hydration the microstructure appears almost the same as the higher water-to-cement ratio, except that there is much more intergrowth of the columnar zones of adjacent grains.

Table 2.3. Comparison of Permeabilities of Rocks and Cement Pastes

Kind of rock	Permeability of rock (darcys)	Water-cement ratio*
Dense trap	$2.57 \times 10^{-9}$	0.38
Quartz diorite	$8.56 \times 10^{-9}$	0.42
Marble	$2.49 \times 10^{-8}$	0.48
Marble	$6.00 \times 10^{-7}$	0.66
Granite	$5.57 \times 10^{-6}$	0.70
Sandstone	$1.28 \times 10^{-5}$	0.71
Granite	$1.62 \times 10^{-5}$	0.71

\* Water-cement ratio of mature paste having same permeability as rock.

capillary porosity leads to a more permeable solid. By choosing a lower water-to-cement ratio the permeability may be decreased to very small values.

A cement paste with a water-to-cement ratio of approximately 0.3 is schematically shown in Figure 2.4 and it is readily apparent that this paste is less porous than that in Figure 2.3. Powers (7) reports the coefficient of permeability of a paste with zero capillary porosity has been measured to be about  $7 \times 10^{-11}$  darcys.\* The design of low permeability cement paste is generally dependent on choosing a low water-to-cement ratio. To apply this to ferro-cement the sand used for the mortar must be free from porosity, and the water-to-cement ratio

---

\* A flow rate of  $1 \text{ cm}^3$  per second through an area of  $1 \text{ cm}^2$  under a pressure gradient of 1 atm per cm with a fluid having a viscosity equal to 1 centipoise equals 1 darcy.

must be as low as possible. Powers (7) has compared the permeabilities of rocks and cement pastes and he produced Table 2.3, which shows that the permeability of the pastes can be less than most natural rocks. The sand grains used in ferro-cement mortars would usually have less permeability than the values for natural rocks given in Table 2.3 since much of that permeability is probably due to micro cracking and other imperfections in larger samples of material.

## 2.2 Factors Leading to the Galvanic Cell Problem

One of the primary roles of the mortar in ferro-cement is to cover and protect the reinforcing steel from corrosion and other environmental effects. Portland cement mortar will protect reinforcing steel if the mortar cover is thick, the permeability of the mortar is low, and the mortar-steel interface is free of discontinuities and voids. As discussed above the permeability of the mortar can be controlled, but the thin layers of mortar may not be sufficient to give protection in all cases.

In an aggressive environment, such as that encountered by ferro-cement in its highly corrosive marine application, the mortar protection of the steel may be too low to prevent excessive corrosion. The danger of corrosion is highly enhanced in ferro-cement by the extremely thin protective cover of mortar over the steel reinforcement. Also, it is known that the alternating conditions of wetting and drying of marine structures through sea spray and marine fog creates additional exposure hazards (8).

In order to minimize absorption, the exterior of a ferro-cement



hull can be covered with a rather impermeable film of epoxy paint. However, this coating is subject to abrasion, deterioration, porosity, etc., and cannot be considered to be 100% effective. Any uncoated area will be subject to intensified local corrosion. Absorption or penetration will also occur from the interior of a hull structure from an accumulation of bilge water or other collected pools of water. This water will not only contribute directly to the corrosion of the steel but also indirectly by leaching out the natural protective constituents of mortar when the water is either high in sulfates (sea water) or when the water is soft (rain water).

From the preceding discussion there are four main reasons for using *galvanized* wire or mesh in ferro-cement.

1. When the reinforcing is exposed to the elements for lengthy periods before the mortar is placed, galvanized wire will resist corrosion better than ordinary steel.
2. Field experiences and experiments at the University of California have shown that concrete with galvanized reinforcement resists an aggressive environment better and longer than concrete reinforced with black steel (9).
3. Once corrosion is initiated in ferro-cement, the zinc will corrode preferentially and will furnish cathodic protection to the steel. Work of Ishikawa, Cornet, and Bresler has shown that galvanized steel is anodic to black steel in concrete by about 0.5 volts and furnishes galvanic protection to steel in concrete in much the same way as it does in the atmosphere (10). Furthermore, corrosion may be slower in starting with

galvanized steel, because zinc is somewhat more tolerant of chlorides than iron in the alkaline concrete environment.

4. Since the protective mortar cover is very thin (about  $\frac{1}{8}$ -in) in ferro-cement, the possibility of corrosion is very high. Therefore, black steel is very vulnerable, especially if any part of the steel reinforcement, bars or mesh, is left unprotected at the surface, for they would become focal points for the initiation of corrosion.

These are good reasons to use *galvanized* steel mesh in ferro-cement, and the authors of this report recommend its use. The problems discussed below are not solved by just removing the galvanized coating on the steel mesh.

### 3. GALVANIC CELL PROBLEM

#### 3.0 The Problem

In all the literature surveyed, there has never been any mention of the severe effects in ferro-cement caused by the presence of the dissimilar metals employed with fresh portland cement mortar (practical applications do not reveal the problem). The two dissimilar metals are the zinc coating of the galvanized mesh and the iron in the ungalvanized steel bars. These metals in the presence of an electrolyte, in the form of portland cement mortar, create an electrochemical (or galvanic) cell, as represented in Figure 3.1. Electron current flows from the zinc anode to the iron cathode with the electrolyte completing the circuit.

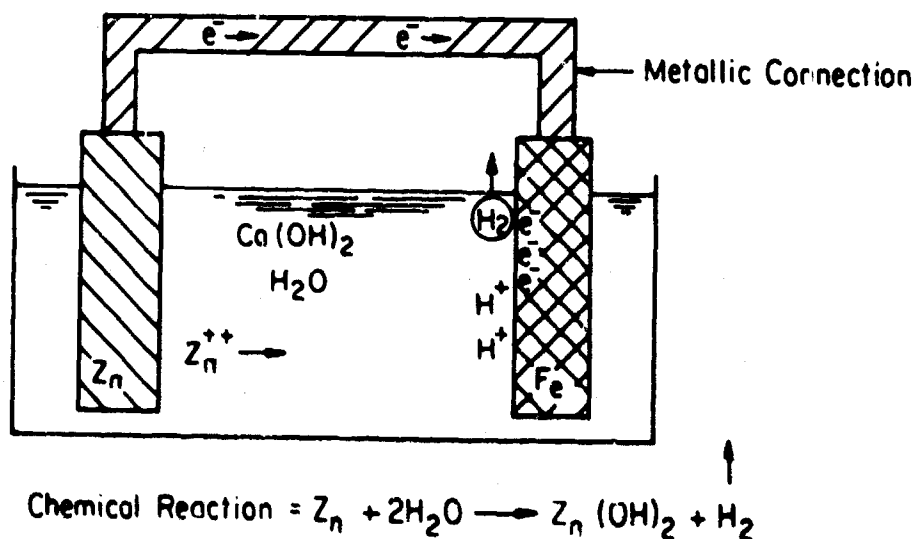


Figure 3.1. Schematic representation of a zinc-iron galvanic cell.

This galvanic cell action is present in hardened and fully cured mortar, but in this case it does not necessarily pose a problem because very low electron currents are present. As a matter of fact, the use of zinc has the benefit of providing cathodic protection to the steel as explained above. However, a very severe problem does exist when the mortar is fresh. Up until the time the mortar sets, very large electron currents flow from the zinc anode to the iron cathode, where hydrogen ions acquire electrons and form hydrogen atoms. The hydrogen atoms combine to form molecules of hydrogen gas ( $H_2$ ), which is liberated along the surface of the black steel cathode as schematically represented in Figure 3.2.

The generation of this gas causes an expansive pressure on the mortar surrounding the bars and creates a gas filled void along the

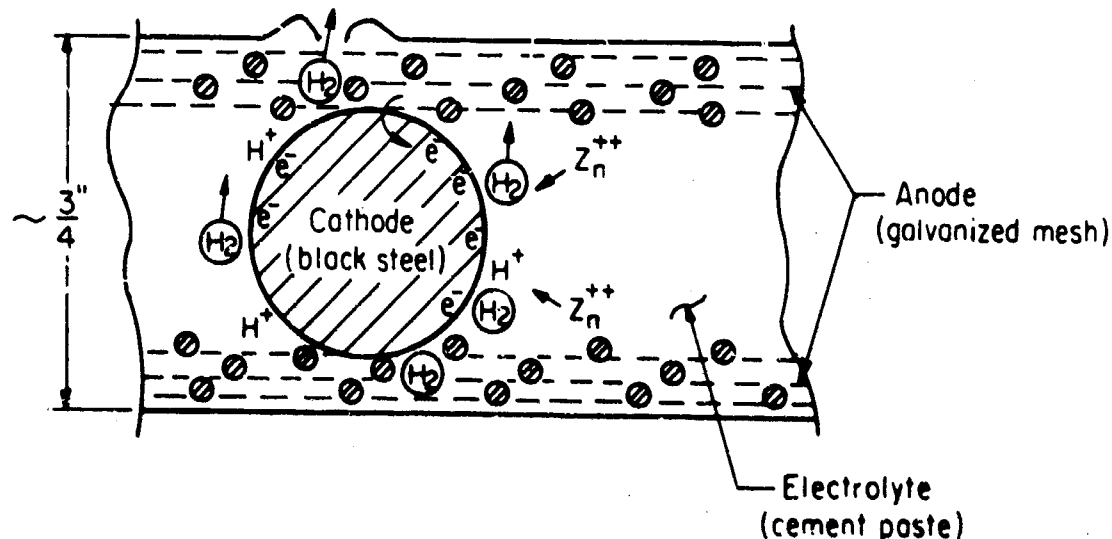


Figure 3.2. A cross section of ferro-cement schematically showing the galvanic cell between galvanized mesh and black steel reinforcing bar.

entire surface area of the cathodic steel bars. Therefore, after the cement paste has set, a continuous disrupted region will exist at the mortar-steel bar interface.

There are three very important deleterious results:

1. Poor mortar to bar bond strength - both chemical and mechanical (frictional).
2. Hydrogen embrittlement of the steel.
3. High corrosion probability from the continuous void along the bars.

Item one: The poor bond strength would affect the overall strength of the ferro-cement, that is, the impact strength, the tensile strength, and the strength in flexure. Although the extremely poor bond reduces the overall strength, many successful ferro-cement boats have been built with an apparently adequate strength - at least initially.

Item two: When high tensile steel is charged with atomic hydrogen (hydrogen ion in contact with steel) under the condition of cathodic charging, the steel is susceptible to hydrogen embrittlement. This condition could lead to a brittle failure of the steel.

Item three: The continuous voids along the bars will invite accelerated corrosion effects, particularly since there is little mortar cover in ferro-cement. Normally, in the extremely corrosive marine environment at least a 3-in concrete cover is recommended (11). It is likely that the accelerated corrosion effect is the most critical result of the galvanic cell action.

A severe deterioration of the overall strength of ferro-cement would be the end result of items 2 and 3 above. It is beyond any

doubt that the problem described is very serious and undesirable in ferro-cement.

### 3.1 Recognition of the Problem

Since the black steel bars are imbedded in the middle of the ferro-cement shell, there would generally be at least a  $\frac{1}{4}$ -in of mortar cover over the black steel ( $\frac{1}{8}$ -in cover over the galvanized mesh). This cover or layer of mortar would usually be sufficient to suppress the emergence of the hydrogen gas at the surface. In actual boat building practice the shell would normally have a more or less vertical surface, which would have the effect of increasing the suppressive force of the mortar over that of the expanding gas. This is the reason why this galvanic cell problem has gone unnoticed and unreported.

If a ferro-cement panel were to be placed horizontally, the gas could emerge at a soft or less dense location. This possibility would be guaranteed if the panel were to be vibrated or shaken, because the gas would then be agitated through the fresh mortar to the surface. There the gas would pop out in the form of an eruption or bubble, resulting in a miniature crater as shown in Figure 3.2.

Indeed, it was through the horizontal fabrication of ferro-cement test panels, as described in the preceding paragraph, that the galvanic cell problem was first recognized by the authors during their research work in 1970. The acuteness of this problem was paramount while conducting extensive tests for strength and while experimenting with unique configurations of ferro-cement (findings of which will be released in subsequent reports).

During this period, test panels  $\frac{1}{2}$ -in to  $1\frac{1}{2}$ -in were fabricated with various layers of galvanized mesh and with  $\frac{3}{8}$ -in black steel bars, sandwiched midway between the mesh on 2-in centers. Vibration of the panels allowed some of the generated gas to escape at various sites of low overhead resistance. At these sites vents formed, and on further vibration they collapsed and then new vents developed. Because the generation of gas is continuous as long as the cement paste has high conductivity, it was found that no amount of vibration at any frequency or amplitude will drive out all the trapped gas.

The surface of the mortar in contact with the reinforcing bars was observed to be highly pitted, but description of these conditions will be delayed until after the solution is described.

### 3.2 Possible Solutions of the Problem

There are a number of possible solutions to the galvanic cell problem described above:

1. Eliminate dissimilar metals
  - a) Use black steel (ungalvanized) reinforcing bars with ungalvanized mesh.
  - b) Use galvanized reinforcing bars with galvanized mesh.
2. Insulate the black steel bars with a protective coating.
3. Chemically passivate or inhibit the galvanic cell action.

The first solution, the most obvious, seemed to offer a good remedy, however, using all ungalvanized steel is not deemed to be desirable, because of the severe threat of corrosion in the highly corrosive marine environment. Marine applications call for a minimum

of three inches of concrete cover over the reinforcement for adequate protection, whereas ferro-cement has only  $\frac{1}{16}$ -in to  $\frac{1}{8}$ -in cover. The use of galvanized bars and mesh was deemed to be a practical solution at a minimal cost, but subsequent tests have indicated that some dissimilar metal characteristics remained because of the different purities of the zinc used in galvanizing or other factors. Care has to be exercised in applying a protective coating to bare spots caused by chipping or cutting of the bars. It should be realized that only mild steel reinforcing bars should be galvanized. However, today's most commonly used reinforcing bars in ferro-cement boat construction are not mild steel, but low carbon, cold drawn steel that is hard (springy) and of high strength (usually over 75,000 psi yield point). Galvanizing this steel will "stress relieve" the steel and cause it to become softer and weaker, therefore, galvanizing of other than mild steel bars is undesirable.

The second solution of insulating the black steel bars could be accomplished with a zinc rich paint or epoxy paint in order to prevent the galvanic currents. Care would have to be exercised in cleaning and preparing the bars for the coating in order to assure a good bond. During fabrication special care would have to be used in order not to scratch or otherwise damage the coating. This would be a tedious and somewhat uncertain method.

The third solution, a chemical cure, was considered to be the most expedient and dependable method if a chemical additive could be found that would eliminate or inhibit the electrochemical cell action. Bresler and Cornet (12) have used chromium ions in solution as a means



of passivating or inhibiting zinc and thereby reducing the galvanic cell effect of zinc and black steel in concrete. They have conducted experiments in which chromium trioxide ( $\text{CrO}_3$ ), also known as chromic oxide, was added in very dilute concentrations of 100 to 300 ppm (parts per million) by weight to that of the water for their concrete mix. All of the mixes with these concentrations proved effective without any loss in the strength characteristics of the concrete.

Each of the possible solutions to the galvanic cell problem has been investigated in this study, but the use of chromium trioxide has proved to be the best solution. In the following sections the results of these experiments will be described and the case for using chromium trioxide will be presented.

#### 4. SOLUTION TO GALVANIC CELL PROBLEM -

##### EXPERIMENTAL RESULTS

#### 4.0 Experimental Methods and Materials

A series of ferro-cement specimens was prepared to investigate the possible solutions to the galvanic cell action described above to take place between galvanized steel mesh and black (i.e., ungalvanized) steel reinforcing bars. Two types of tests, a visual inspection test and a bending strength test, were designed to determine if the addition of chromium trioxide ( $\text{CrO}_3$ ) to the mix of fresh mortar would reduce or eliminate the undesirable effects of the galvanic cell. In addition the use of an all galvanized system, an all black iron system, and an epoxy coated black iron approach were investigated in the same way.

The visual inspection test consisted of two phases. The first phase was the fresh mortar test. Observations were made as to the apparent electrochemical action taking place in freshly cast ferro-cement specimens, with and without the  $\text{CrO}_3$  admixture in the mortar, up until the final setting of the paste. The same test was made for the other treatments as well.

The second phase was the ferro-cement post cure test. This phase of inspection consisted of cutting open the fully cured ferro-cement specimens, casted in phase one, by use of a diamond saw, and then critically examining their internal structure. This test was made for all of the possible solutions to the problem.

Following the visual inspection tests the mechanical properties were investigated using a standard four point bending test (also called a flexure test) to determine what effect the galvanic cell problem has on engineering performance. A limited number of impact studies were also made, but these will be described in a later report.

The materials used in this study were as follows:

1. Mortar

A rich mortar of portland cement and clean, hard, and durable sand was used. A type II portland cement was utilized because it is of a type that can generally be recommended for ferro-cement applications. It is readily available, has fairly slow setting time and has good sulfate resistance.

Mortar Specifications

Cement:	Portland Type II
Sand:	Olympia No. 1
	Fineness modulus: 2.05
	100% passing No. 8 sieve
	15% passing No. 100 sieve
Cement/sand ratio:	0.67
Water/cement ratio:	0.40
Weight of mortar:	142 lb/ft <sup>3</sup> (see calculation below)
Slump:	4-in
Admixture:	Chromium trioxide (as described below)

Chromium trioxide (CrO<sub>3</sub>), also called chromic oxide, was added to the water of the mortar mix (in some of the specimens) in the

concentration of 300 ppm (parts per million) to that of the mix water. A uniform distribution of the chromium ions in the mortar mix was achieved by adding a carefully measured quantity (by weight) of the chromium trioxide crystals to the water weighed out for the mortar batch. Since many engineers involved with ferro-cement are not familiar with cement and concrete it would be useful to present the calculations for batching the chromium trioxide into the mortar.

### Sample Calculation to Determine

#### Batch Weight of CrO<sub>3</sub>

1. Determine the weight of mix water per ft<sup>3</sup> of mortar.

Using the mortar specifications from above and knowing that the specific gravity of cement is approximately 3.15 and that of our aggregate is 2.7, the density of the mortar can be determined.

	Weight (lb)	%	Volume (ft <sup>3</sup> )	%
Aggregate	300	51.8	1.78	43.5
Cement	200	34.4	1.02	25.0
Water	80	13.8	1.28	31.5
Totals	580		4.08	

$$\therefore \text{Density of mortar} = \frac{580}{4.08} = 142 \text{ lb/ft}^3.$$

[Aside: This gives 14 sacks (US) cement per yd<sup>3</sup> - a rather rich mix.]

The weight of mix water per ft<sup>3</sup> of mortar is just 13.8% x 142 lb = 19.6 lb/ft<sup>3</sup>.

2.  $\text{CrO}_3$  is to be added in concentration of 300 ppm to mix water and thus:

$$\text{For 1 ft}^3 \text{ Mortar: } \text{CrO}_3 = 300 \text{ ppm} \times \frac{19.6}{10^6} = 0.00588 \text{ lb } (= 2.66 \frac{\text{grams}}{\text{ft}^3})$$

$$\text{For 1 yd}^3 \text{ Mortar: } \text{CrO}_3 = 27 \frac{\text{ft}^3}{\text{yd}^3} \times 0.00588 \text{ lb} = \frac{0.169 \text{ lb}}{\text{ft}^3} (= \frac{71.8 \text{ gm}}{\text{yd}^3})$$

The desired concentration can be obtained by adding a carefully measured amount (by weight) of the  $\text{CrO}_3$  crystals into a small amount of distilled water in order to form a solution. Then a measured amount of this  $\text{CrO}_3$  solution is added to the mix water of each batch. An example will serve to illustrate the point.

#### Example

A total of 3  $\text{yd}^3$  of mortar is to be used on a job. Batches of 4  $\text{ft}^3$  are to be mixed at one time.

1. Total amount of  $\text{CrO}_3$  needed:

$$3 \text{ yd}^3 \times 71.8 \text{ grams/yd}^3 = 215.4 \text{ grams}$$

2. A solution of  $\text{CrO}_3$  is made by adding 215.4 grams of  $\text{CrO}_3$  to 500 ml of distilled water.

3. Number of milliliters of  $\text{CrO}_3$  solution needed per 4  $\text{ft}^3$  batch:

$$\text{CrO}_3 \text{ Solution} = \frac{\text{ft}^3/\text{batch}}{\text{total ft}^3} \times 500 = \frac{4}{81} \times 500 = \underline{24.7 \text{ ml.}}$$

Therefore, in this example 24.7 ml of  $\text{CrO}_3$  solution are added to the mix water needed for a batch of 4  $\text{ft}^3$  of mortar. The use of mixed units of the metric and english systems was chosen because the smaller volume and weight scales are often in the metric system.

Table 4.1. Mortar Mix

Mortar	Water (lb)	$\text{CaO}_3$ (gms)	Cement (lb)	Sand (lb)	Total Weight (lb)
1 ft <sup>3</sup>	19.6	2.66	48.8 (0.52 sacks, US)	73.6 (SSD)	142
1 yd <sup>3</sup>	528	71.8	1,320 (14 sacks, US)	1,980 (SSD)	3,830
US sack = 94 lb SSD = Saturated Surface Dry					

The mortar used in this study can be summarized in Table 4.1.

## 2. Reinforcement (Steel)

A standard  $\frac{3}{8}$ -in diameter reinforcing bar was used in these studies and two types of steel mesh. The specifications for these materials are as follows:

### Reinforcing bar No. 3 ( $\frac{3}{8}$ -in) deformed

- a) Black steel (ungalvanized)
- b) High tensile strength (60,000 psi yield point)
- c) Weight: 0.376 lb/ft
- d) Weight if placed on 2-in centers in ferro-cement: 2.256 lb/ft<sup>2</sup>

### Hardware cloth (steel mesh) No. 2

- a) Square openings: 2 squares/inch
- b) 19 gage (0.041-in diameter, 0.00132-in<sup>2</sup> area)
- c) Galvanized
- d) Welded woven wire
- e) Weight: 0.244 lb/ft<sup>2</sup>

Chicken wire (aviary netting)  $\frac{1}{2}$ -in

- a) Hexagonal openings: 2 openings/in
- b) 22 gage (0.0286-in diameter, 0.000642-in<sup>2</sup> area)
- c) Galvanized
- d) Welded twisted wire
- e) Weight: 0.124 lb/ft<sup>2</sup>

### 3. Specimens

The visual inspection test specimens were 18-in x 18-in and consisted of two thicknesses with different laminations. One thickness of a normally employed ferro-cement cross section,  $\frac{3}{4}$ -in, and a smaller thickness,  $\frac{1}{2}$ -in, were tested.

The reduced cover of mortar on the  $\frac{1}{2}$ -in thick ferro-cement specimen caused a reduction of constrictive pressure over the sites of the generated hydrogen gas (at the mesh-bar interface). This allowed more visible indication of the effect of the liberation of the gas within the specimen.

The visual inspection specimens were fabricated as follows: Plywood molds were used in the fabrication in order to achieve a uniform thickness, the sides of the molds being of the correct height. The steel mesh and bars were wired tightly together through holes drilled in the bottom of the molds.

The mortar was impregnated into this tight mesh by force of a trowel and by vibration of the molds on a vibrating table. Vibration (approximately 60 cps, variable amplitude) of the specimens lasted approximately 20 seconds. The specimens were then troweled smooth and left undisturbed.

1. Specimen with  $\frac{3}{4}$ -in laminate (shown in Figure 4.1)
  - a)  $\frac{3}{4}$ -in x 18-in x 18-in
  - b) 6 layers of No. 2 hardware cloth
  - c) 8 ea. No. 3 steel bars on 2-in centers

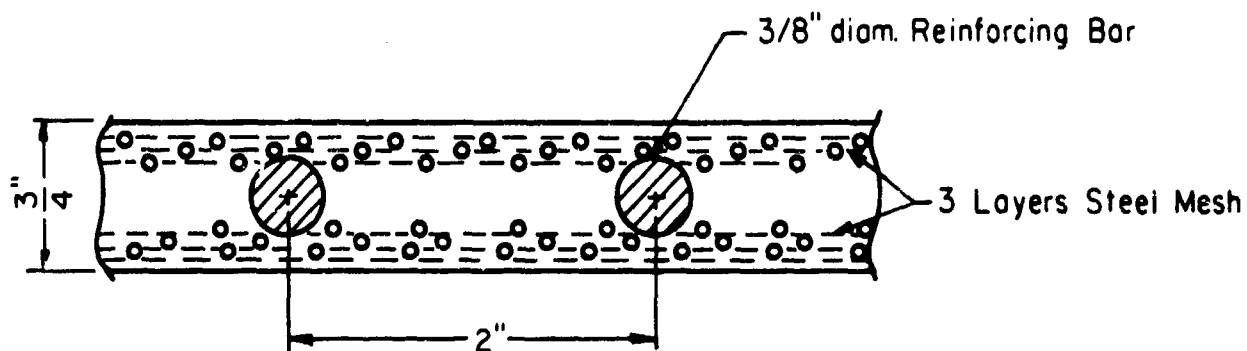


Figure 4.1.  $\frac{3}{4}$ -in ferro-cement visual inspection specimen (cross section), scale 1:1.

2. Specimen with  $\frac{1}{2}$ -in laminate (shown in Figure 4.2)
  - a)  $\frac{1}{2}$ -in x 18-in x 18-in
  - b) 4 layers of No. 2 hardware cloth
  - c) 8 ea. No. 3 steel bars on 2-in centers

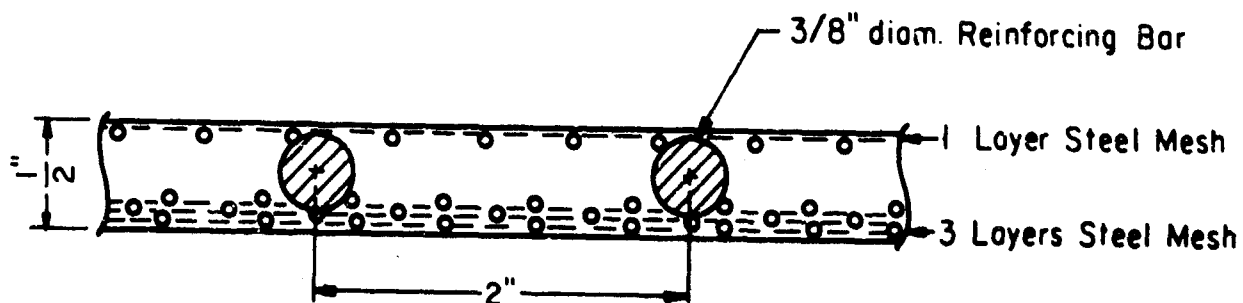


Figure 4.2.  $\frac{1}{2}$ -in ferro-cement visual inspection specimen (cross section), scale 1:1.



The two sets of specimens (with and without the  $\text{CrO}_3$  admixture) were cast one after the other in separate batches of mortar. The batch with  $\text{CrO}_3$  followed the mixing and casting of the batch without  $\text{CrO}_3$  by just a few minutes. Except for the addition of the  $\text{CrO}_3$  admixture, the batches, the mixing, and the casting were identical for both sets of specimens. The other specimens employing epoxy seal, etc., were prepared in the same fashion but at a later time.

The curing was accomplished in two steps:

1. Air cure at approximately 75 degrees Fahrenheit until the mortar set - approximately 2 hours, then
2. Wet cure, 73 degrees Fahrenheit at 100% relative humidity for 28 days (molds stripped on second day).

This curing was chosen in order to most closely represent the curing employed in the field.

The bending test specimens were 6-in x 24-in with a nominal  $\frac{3}{4}$ -in thickness. Two types of reinforcing laminates were employed. One laminate had 6 layers of hardware cloth, and the other had 8 layers of chicken wire. More layers of chicken wire were needed than layers of hardware cloth for the same  $\frac{3}{4}$ -in thickness because of the different gages of wire (see paragraph above for specifications of the reinforcements).

1. Specimen with hardware cloth

- a)  $\frac{3}{4}$ -in x 6-in x 24-in
- b) 6 layers of No. 2 hardware cloth
- c) 3 ea. No. 3 steel bars

2. Specimen with chicken wire

- a)  $\frac{3}{4}$ -in x 6-in x 24-in
- b) 8 layers of  $\frac{1}{2}$ -in chicken wire
- c) 3 ea. No. 3 steel bars

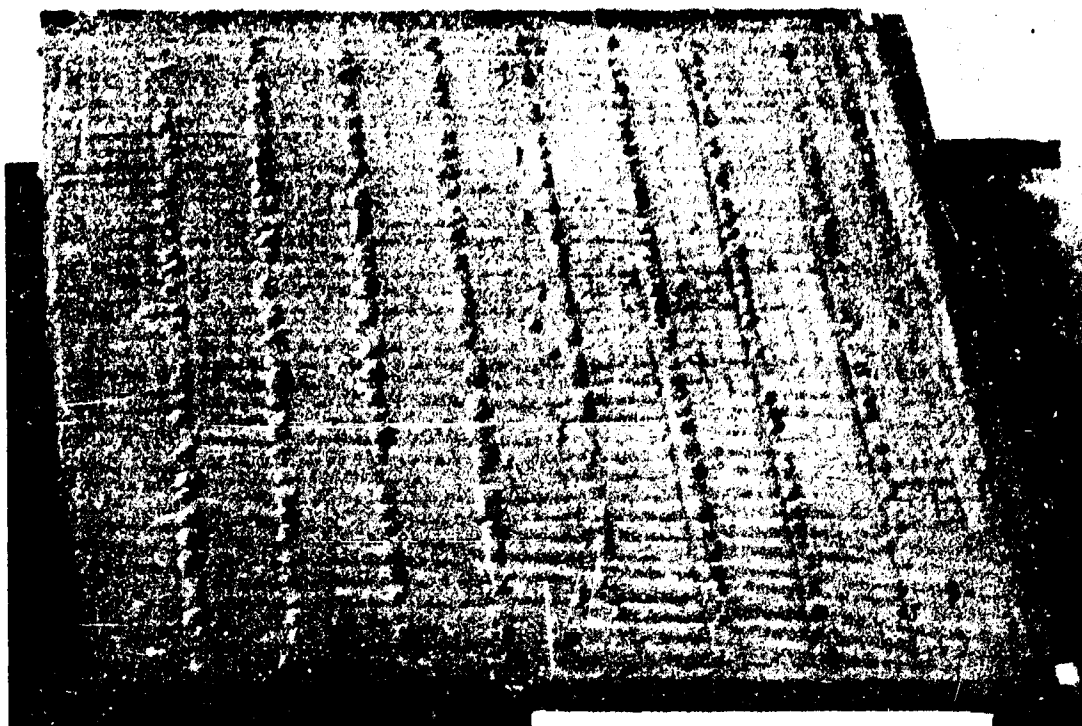
The same fabrication and curing techniques were followed for both specimens.

#### 4.1 Experimental Results

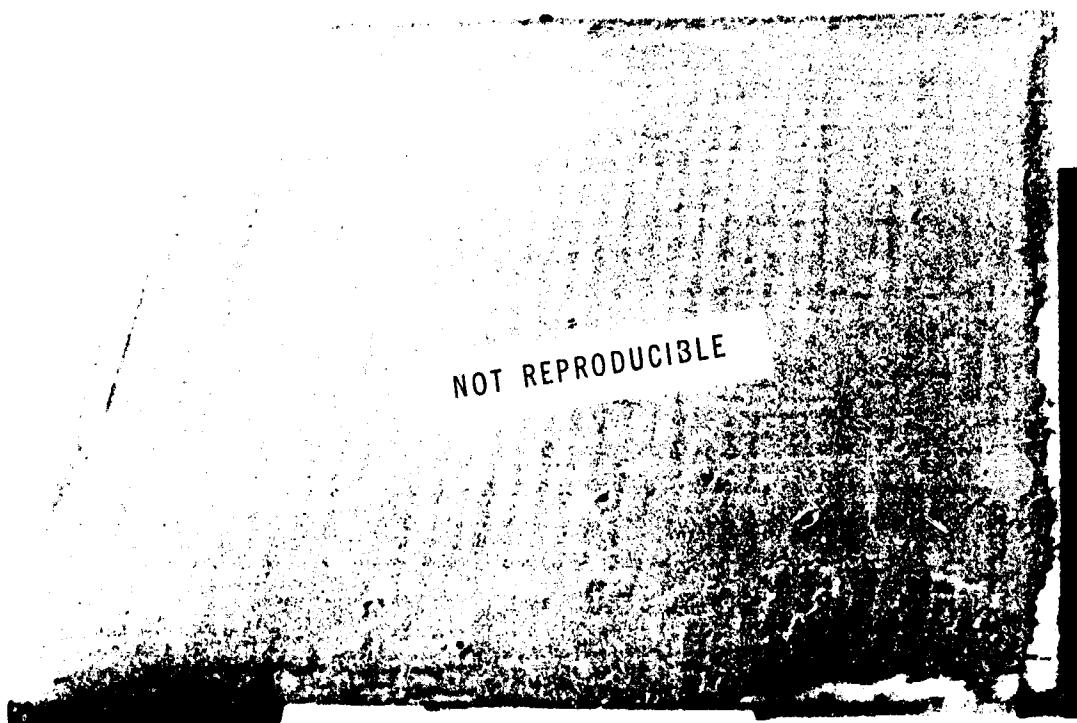
The visual observations recorded during the first hour after the preparation of four test panels are shown in Table 4.2. Two panels

Table 4.2. Visual Observations of Galvanic Cell Activity on Fresh Ferro-Cement Panels both with and without  $\text{CrO}_3$ .

Time After Casting	Ferro-Cement Specimens			
	Without $\text{CrO}_3$		With $\text{CrO}_3$	
	$\frac{1}{2}$ -in	$\frac{3}{4}$ -in	$\frac{1}{2}$ -in	$\frac{3}{4}$ -in
10-15 min	Bubbles formed rapidly in the mortar over the length of each reinforcing bar. Bubbles approx $\frac{1}{2}$ -in dia.	Sputtering eruptions (4 to 5) with vents approx $\frac{1}{8}$ - $\frac{1}{4}$ -in dia.	No bubbles or eruptions	No bubbles or eruptions
30 min	Bubbles were continuous, approx 0 to $\frac{1}{2}$ -in apart along the entire length of each bar. Only a few of these bubbles would burst and then bubble up again. Bubbles also formed over the black steel tie wires holding the mesh together.	Vents well formed (9 to 10 ea) at random sites over a reinforcing bar.	No bubbles or eruptions	No bubbles or eruptions
60 min	No new bubbles. Many of the bubbles had flattened and had cracks in their tops, allowing the gas to escape. <i>See Figure 4.3 (a)</i>	Vents well formed (11 ea) up to $\frac{1}{4}$ -in dia. <i>See Figure 4.3 (b)</i>	No bubbles or eruptions <i>See Figure 4.3 (c)</i>	No bubbles or eruptions <i>See Figure 4.3 (d)</i>

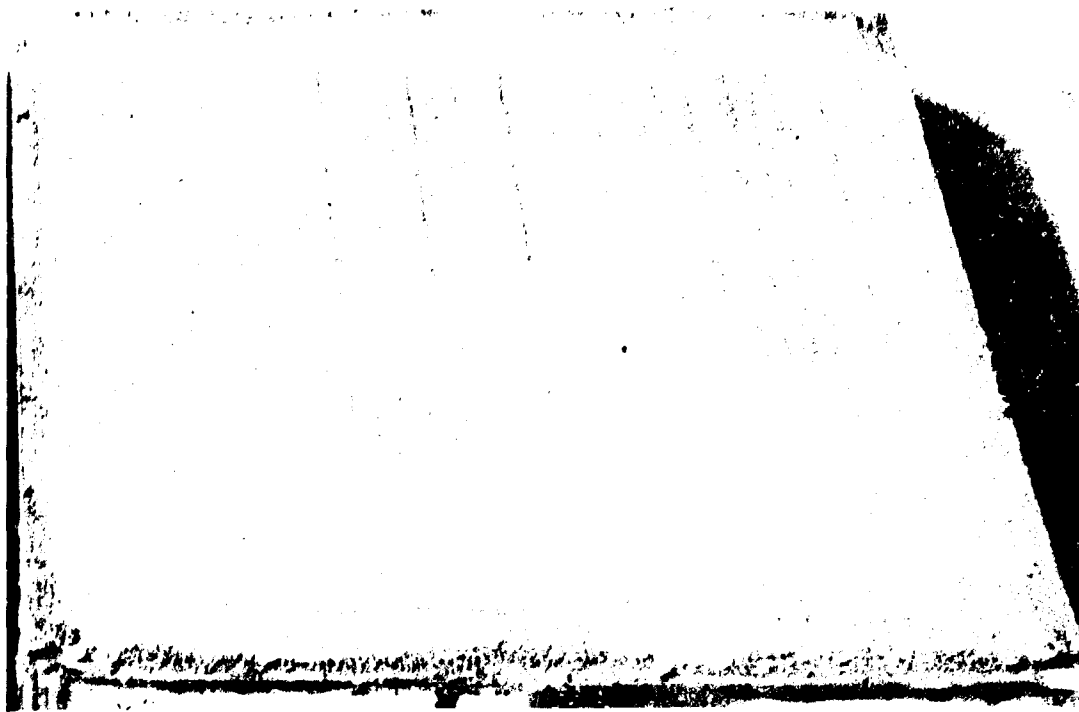


(a)

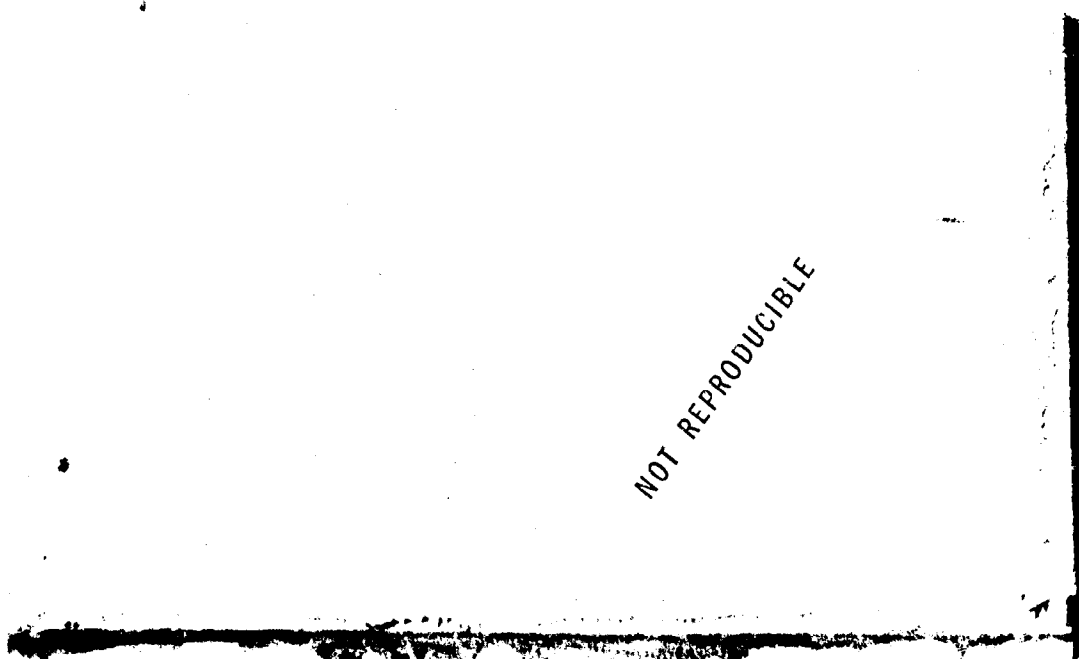


(b)

Figure 4.3. Ferro-cement panels one hour after casting showing the effects of  $\text{CrO}_3$  in suppressing the galvanic cell activity, (a)  $\frac{1}{4}$ -in thick specimen showing rows of bubbles along the reinforcing bars caused by the evolution of hydrogen, (b)  $\frac{3}{4}$ -in thick specimens showing the rather large vents randomly distributed over the surface.



(c)



(d)

Figure 4.3. (continued from opposite page)... (c)  $\frac{1}{2}$ -in thick specimen with  $\text{CrO}_3$  shows no bubbles like those shown in (a), (d)  $\frac{3}{4}$ -in thick specimen with  $\text{CrO}_3$  shows no vents like those in (b).

contained  $\text{CrO}_3$  and showed no bubbling or eruptions on the surface at all. This contrasted with the two panels without  $\text{CrO}_3$  which exhibited active bubbling or spurting. The four panels are shown in Figures 4.3 (a b c d), and it is clear that the addition of  $\text{CrO}_3$  has reduced the galvanic cell sufficiently to prevent the hydrogen bubbles from breaking through to the surface. This is particularly evident if the two panels with only one layer of mesh are compared, Figure 4.3 (a) and (c). There is little resistance for the bubbles to break through and yet the specimen with  $\text{CrO}_3$  showed no bubbling at all. Note that the bubbles are clearly visible on the test panel without  $\text{CrO}_3$  shown in Figure 4.4 after the complete curing process; this is the same panel shown in Figure 4.3 (a) one hour after being cast. The test panels were cured, as described above, for 28 days at 100% relative humidity.

The fully cured ferro-cement specimens were cut with an 18-in diamond saw, both at a right angle and longitudinally to the reinforcing bars, in order to observe the bonding characteristics of the mortar to the steel reinforcing bars. The longitudinal cuts were made top and bottom to the bars down to the surface of the bars, thereby allowing the ferro-cement to be "opened up" along the length of the bars. This allowed individual bars to be removed from the specimens.

The specimens *without*  $\text{CrO}_3$  exhibited a continuous void along the entire length and circumference of the bars. There was evidence of very little contact between the mortar and steel. The surface of the mortar surrounding the bars was pocked, giving a spongy appearance as shown in Figure 4.5. Few smooth areas could be found that would indicate that contact or bond had been made by the mortar to the bars. Entrapped

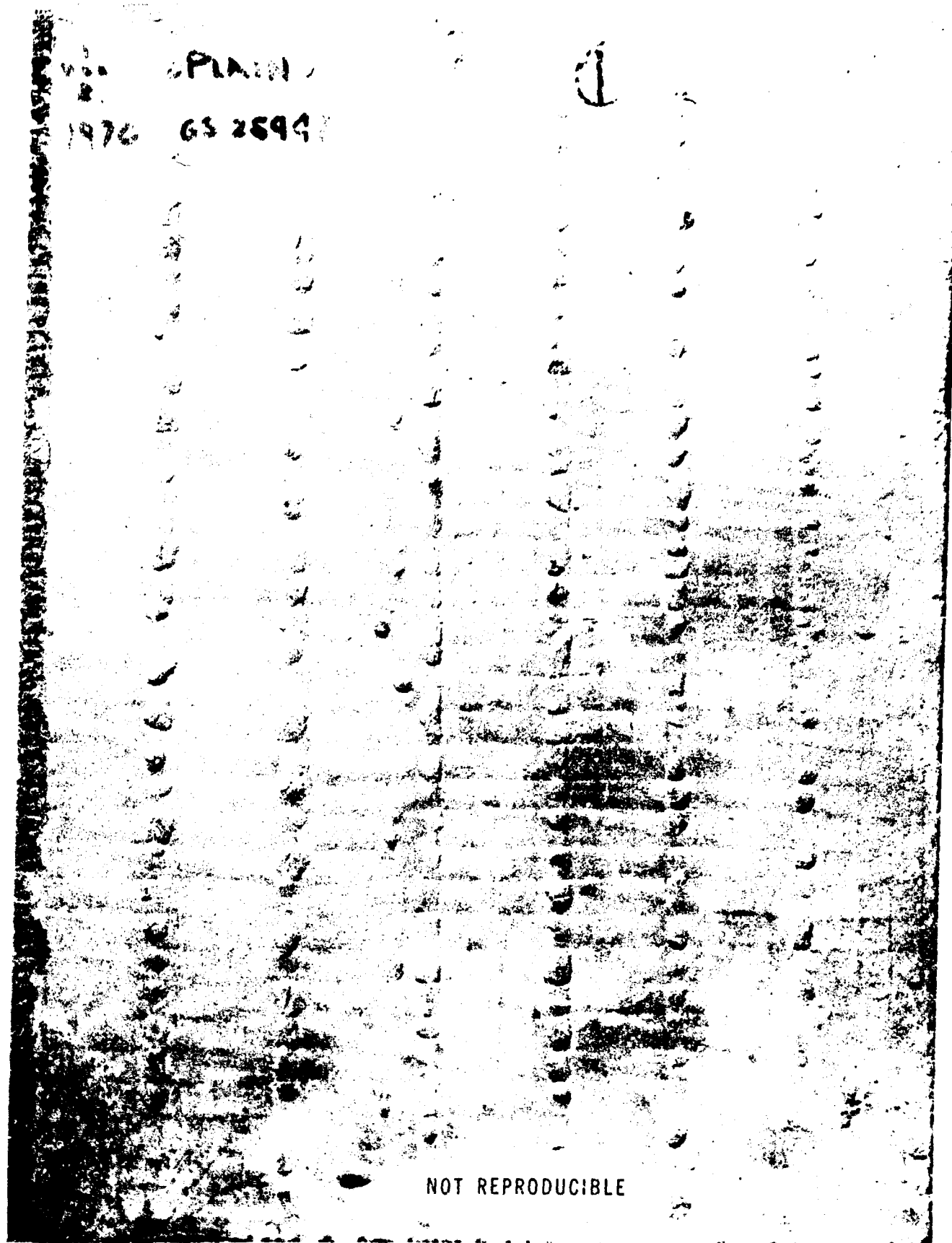


Figure 4.4. The rows of bubbles along reinforcing bars shown in Figure 4.3 (a) are retained in the final cured panel after 28 days moist cure.

hydrogen gas had completely encircled the bars and forced the mortar back from the surface of the bars.

The specimens *with* the  $\text{CrO}_3$  admixture revealed a perfect impression of the deformed steel bars in the mortar. An excellent, void free bond existed along the entire length of each bar inspected. This is graphically illustrated in Figure 4.5 where the pocked surface of the mortar without  $\text{CrO}_3$  is shown alongside that with  $\text{CrO}_3$ .

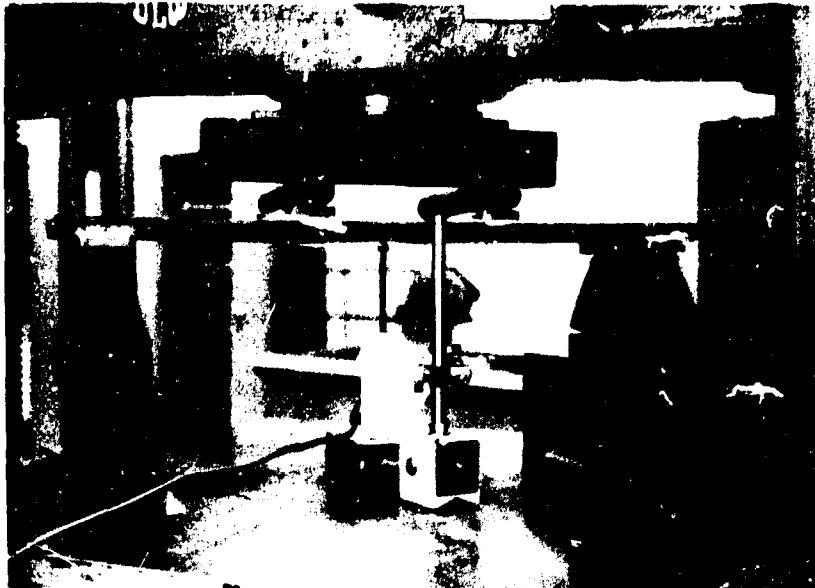
The flexure tests were conducted on four ferro-cement panel specimens as described above. Two of the specimens contained  $\text{CrO}_3$  and two did not. A Baldwin Universal Testing Machine of 60,000 pounds capacity was used with a linear differential transformer placed at mid-span to measure the deflection. A typical flexure test is shown in Figure 4.6 (a b) with a  $\frac{1}{2}$ -in thick ferro-cement specimen in place. The specimen shown in Figure 4.6 (b) has a deflection of 1.5-in and the stress in the outer fiber is 4,816 psi. That specimen was made with only mesh and no reinforcing bars. The spacing of the loading points is 7-in on centers with load transmitted to the specimen through four  $\frac{1}{4}$ -in x 2-in x 6-in steel bearing plates set in place with a quick-drying, high strength gypsum plaster (hydrostone). The deflection was recorded continuously with an electronic x-y recorder and the loading rate was 240 lb/min until ultimate failure.

The load deflection curves for the flexure tests of the specimens with and without  $\text{CrO}_3$  are shown in Figure 4.7 and it is apparent that the presence of  $\text{CrO}_3$  makes a difference in the mechanical behavior of these panels. Both the apparent modulus and the ultimate strength are increased by using  $\text{CrO}_3$ . The numerical values for these quantities

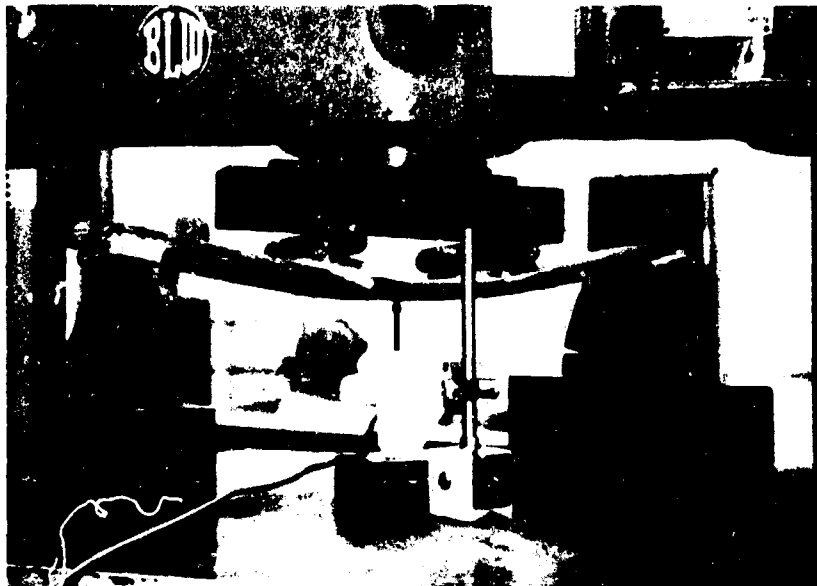


Figure 4.5. The surface of the mortar without  $\text{CrO}_3$  is shown to be spongy where it was in contact with the reinforcing bar, but to be smooth in the case where  $\text{CrO}_3$  was added to the mortar.





(a)



(b)

Figure 4.6. A typical flexure test is shown where the load is applied to third points of the specimen and the strain is measured at mid-span. (a) No load is applied to the  $\frac{1}{2}$ -in thick ferro-cement specimen. (b) A deflection of 1.5 inches is shown for the same specimen under test where the stress was 4,816 psi in the outer fiber.

Table 4.3. Flexure Test Results for Ferro-Cement with and without  $\text{CrO}_3$ .

Ferro-Cement Specimen $\frac{3}{4}$ -in x 6-in x 24-in		Apparent Modulus of Elasticity (determined at 50% ultimate load) (psi)	Ultimate Strength		
			Deflection (in)	Load (lb)	Stress (psi) (outer fiber)
Hardware cloth reinforcement	With $\text{CrO}_3$	$3.65 \times 10^6$	0.975	2,460	15,300
	Without $\text{CrO}_3$	$2.2 \times 10^6$	1.0	1,550	9,650
Chicken wire reinforcement	With $\text{CrO}_3$	$3.88 \times 10^6$	0.775	2,116	13,200
	Without $\text{CrO}_3$	$1.94 \times 10^6$	0.950	1,485	9,250

are given in Table 4.3 and a direct comparison can be made. The apparent modulus of the hardware cloth sample was increased by 1.6 from  $2.2 \times 10^6$  psi to  $3.65 \times 10^6$  psi and that of the chicken wire was increased by a factor of 2 from  $1.94 \times 10^6$  psi to  $3.88 \times 10^6$  psi by the addition of  $\text{CrO}_3$ . The ultimate strength was also greatly increased by the addition of  $\text{CrO}_3$ .

It is interesting to note that the specimen with 6 layers of hardware cloth compared almost identically to the specimen with 8 layers of chicken wire for the specimens *without*  $\text{CrO}_3$ , see Figure 4.7. The ultimate stress of these specimens, over 9,000 psi, were at the very top of the ultimate stress range for ferro-cement (approximately 5,000 - 9,000 psi) as reported by previous investigators.

The ferro-cement specimens *with*  $\text{CrO}_3$  exhibited 59% and 43% greater

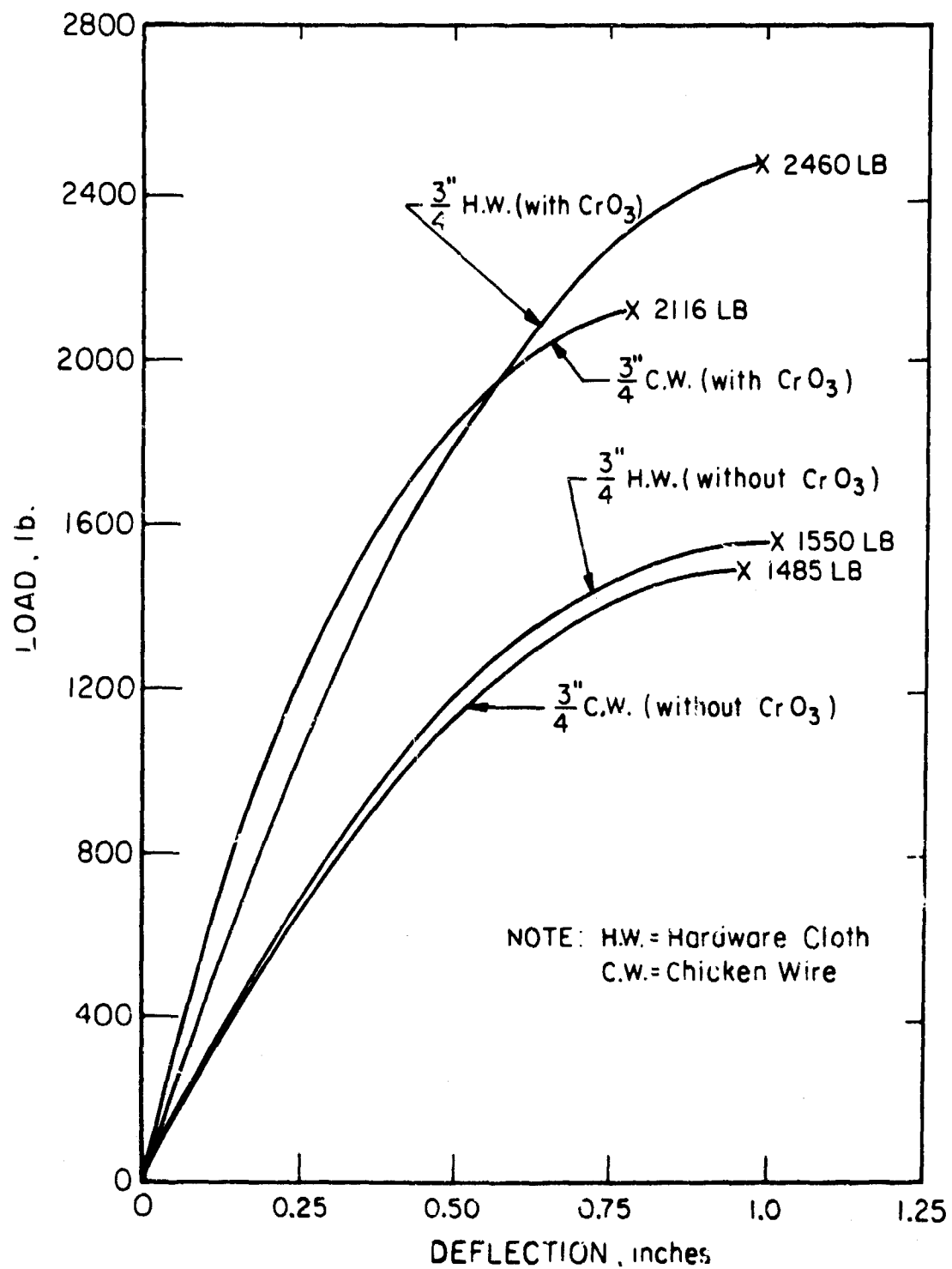


Figure 4.7. The load-deflection curve for the flexure tests of specimens with and without  $\text{CrO}_3$ . The specimens with  $\text{CrO}_3$  show substantially greater stiffness as well as ultimate strength.

strengths in flexure respectively for the hardware cloth and for the chicken wire reinforcements than for their counterparts *without*  $\text{CrO}_3$ . These strengths corresponded to stresses of 15,300 psi and 13,200 psi respectively. Subsequent tests with welded wire fabric show even better strengths using  $\text{CrO}_3$  and these will be reported later.

The results of the visual tests showed that the chemical bond and the mechanical friction between the steel bars and the concrete was very low for ferro-cement *without*  $\text{CrO}_3$ . This fact was confirmed by the bending tests. Therefore, the bond strength (composite strength) between the bars and the concrete was considerably lower for ferro-cement *not treated* with  $\text{CrO}_3$  and greatly reduced the fluctural strength.

It is probable that if plain bars (non-deformed) would be used, those bars would most likely exhibit an even greater tendency to be pulled through the concrete, and failure would occur at even lower loads for mortar *without* the  $\text{CrO}_3$  admixture. This is important for ferro-cement since smooth bar is often used.

The other possible solutions\* to the galvanic cell problem were investigated by visual observations on the freshly cast test panels and by cutting the panels open after a full cure cycle. There was little bubbling observed with any of the other systems and it is interesting that the galvanic cell activity observed without  $\text{CrO}_3$  present is confirmed to be due to the combination of galvanized steel mesh and ungalvanized steel reinforcing bars. This was true for the external examination of the freshly cast panels, but a study of the

---

\* All galvanized system, all black iron system, and an epoxy coated black iron.

internal state of the cured specimens showed that both the all galvanized and all black iron samples had poor mortar/reinforcing-bar surfaces. A photograph of these specimens is shown in Figure 4.8 and it is evident that there has been some activity at the reinforcing bar surface which has made a rough surface. It is probable that this is due to a galvanic cell caused by small differences in the material. Recent tests with welded wire fabric showed that hydrogen gas was evolving from each of the junctions where a weld had been made. Both the all galvanized or all black iron system would be sensitive to small differences in material, and one would never be completely sure that some cells were not established by an unforeseen combination of materials. The  $\text{CrO}_3$  solution appears to be the best solution available. The epoxy coating appeared to work rather well, except that it filled in some of the deformations on the reinforcing bar which would decrease its interlocking with the hardened mortar.

#### 4.2. Microscopic Observations

It is apparent from Figure 4.5 that the use of  $\text{CrO}_3$  gives a much smoother surface of mortar in contact with the reinforcing bars in ferro-cement. Mortar samples from the ferro-cement panels shown in Figure 4.5 were removed and observed in the scanning electron microscope. This type of microscope has been used extensively in previous studies of cement samples (6), and it is particularly useful for these studies because it has a large depth of field and magnification from as low as 25x to as much as 200,000x with a resolution of approximately 250 Å.

The rough surface of the sample without  $\text{CrO}_3$  is shown in a mosaic

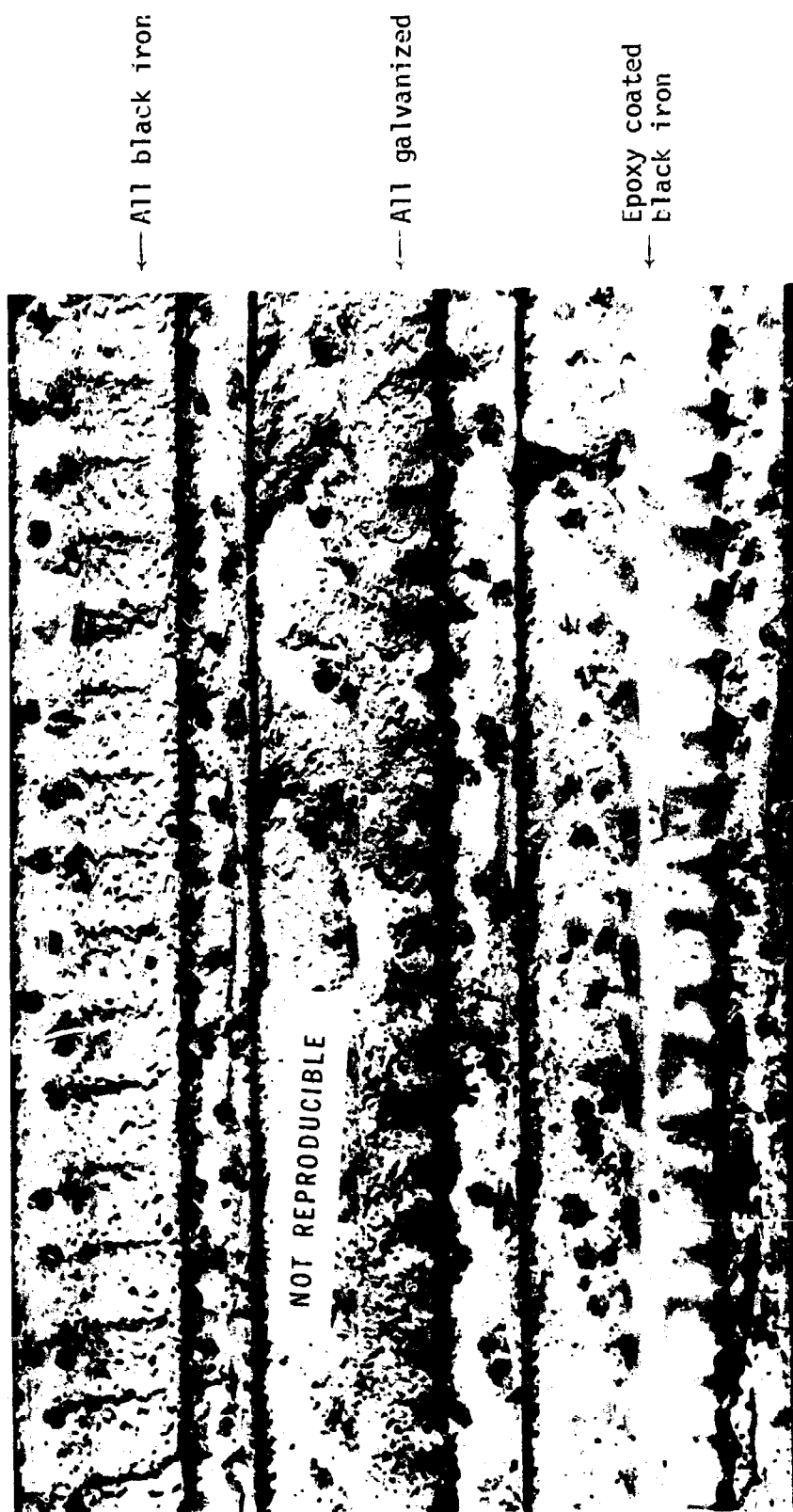


Figure 4.8. The surface of the mortar is shown to be somewhat spongy where it was in contact with the reinforcing bar in both the all black iron and all galvanized systems. Note that the epoxy coated surface was protected, but that the deformations on the bar are smoothed over.

of micrographs in Figure 4.9. There are so many bubbles near the surface of the reinforcing bar that it is difficult to find zones that were in contact with the steel. There is one contact zone in the foreground of Figure 4.9 that is marked A, but it is small and interrupted by a bubble in the center. A region just to the left of the arrow in Figure 4.9 is shown at higher magnification in Figure 4.10 (a). The surface of the mortar that was in contact with the reinforcing steel is in the upper right hand corner of that figure and it appears relatively smooth. The region to the left in Figure 4.10 (a) is a fracture surface that was created when a piece was chipped out of the sample. This fractured area is visible in Figure 4.9 and probably occurred when the specimen was prepared for the scanning electron microscope. A portion of this fracture surface is shown at higher magnification in Figure 4.10 (b) with broken sand grains visible at several places on the surface. The presence of the broken sand grains means that the cement paste surrounding them is sound and probably unaffected by the evolution of hydrogen at the surface of the reinforcing steel.

A specimen removed from the panel treated with  $\text{CrO}_3$  is shown at low magnification in Figure 4.11 (a) with the surface of the mortar which had been in contact with the reinforcing bar visible in the upper portion of the micrograph. A fracture surface through the mortar is shown in the lower foreground of that figure, and it is free from pores or bubbles. A mosaic of micrographs showing the same region is shown in Figure 4.11 (b) in order to illustrate the smoothness of the interface between the mortar and the reinforcing bar when  $\text{CrO}_3$  is used. A small region marked in the center of Figure 4.11 (b) is shown in



Figure 4.9. A mosaic of scanning electron micrographs showing the rough surface of mortar near the plain steel reinforcing bar when  $\text{CrO}_3$  was not used. The small area marked A and several other areas of similar appearance were in contact with the surface of the steel. The many voids were caused by the evolution of hydrogen at the surface of the steel.



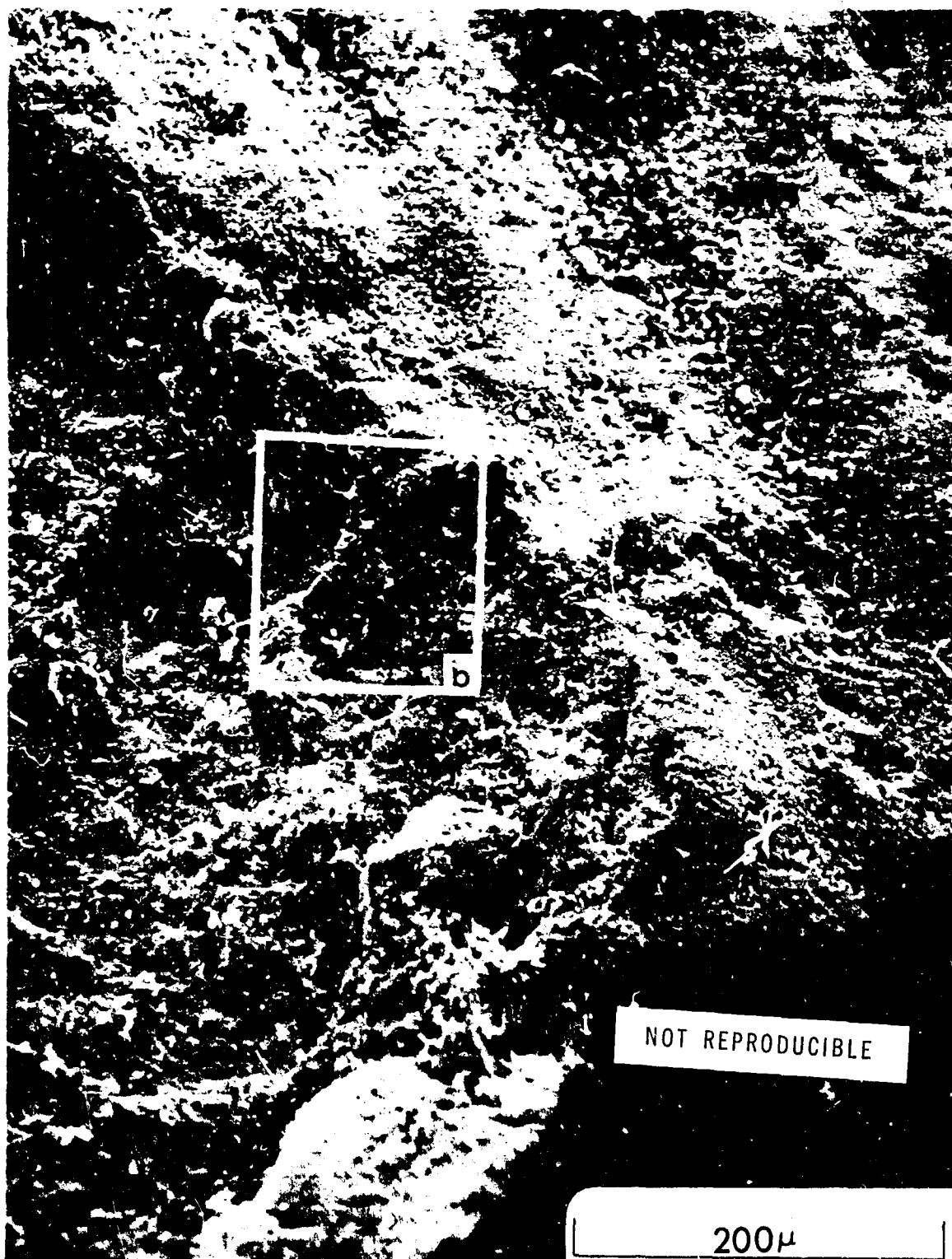


Figure 4.10 (a) A higher magnification micrograph of a region just to the left of the arrow in Figure 4.9. The surface of the mortar that was in contact with the steel is in the upper right hand side of this micrograph.

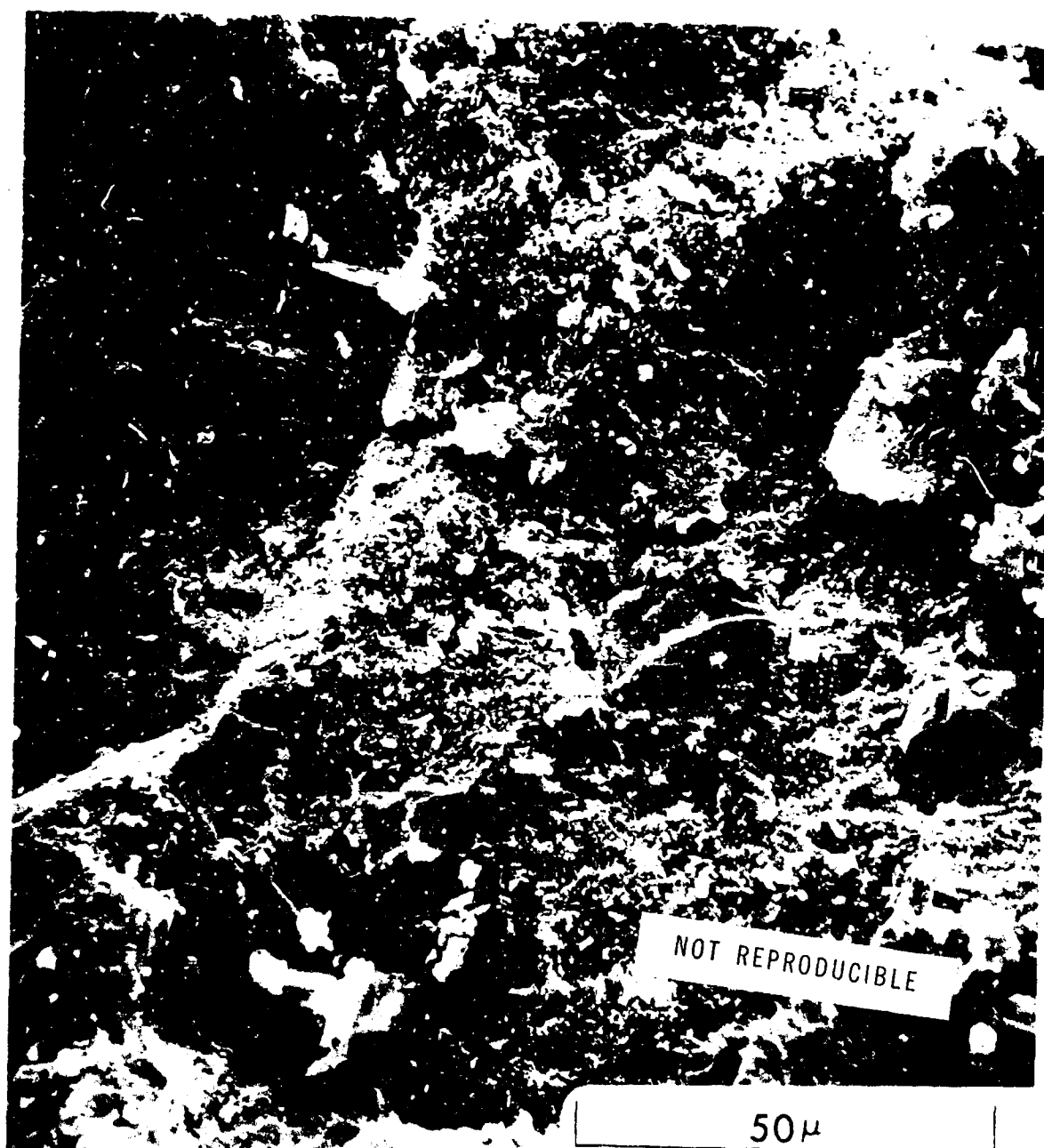


Figure 4.10 (continued from opposite page)... (b) A micrograph of an area marked in (a) which shows the fracture surface of several sand grains. The presence of the broken sand grains means that the cement paste is sound. (Please note that  $1\mu$  corresponds to  $10^{-4}$  cm or approximately  $4 \times 10^{-5}$  in.)

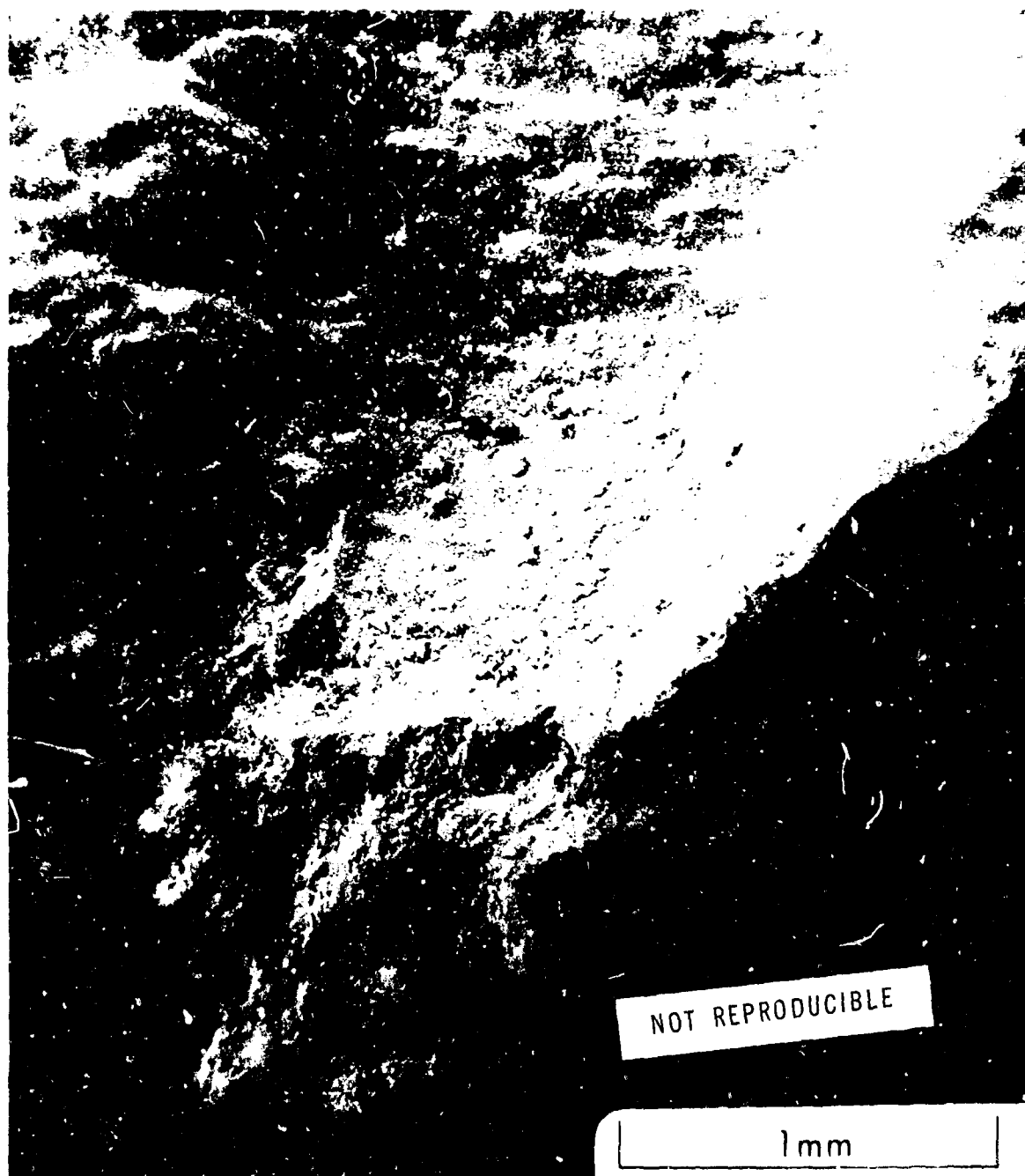
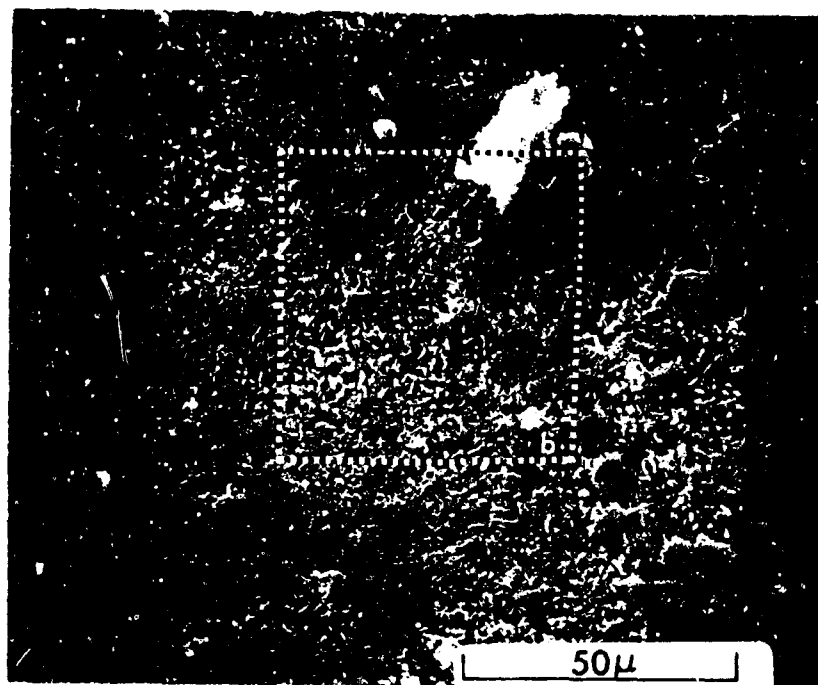


Figure 4.11 (a) A low magnification micrograph showing the surface of the mortar. The surface is smooth and unmarked by bubbles. Notice that there are not any bubbles on the fracture surface through the mortar in the foreground.

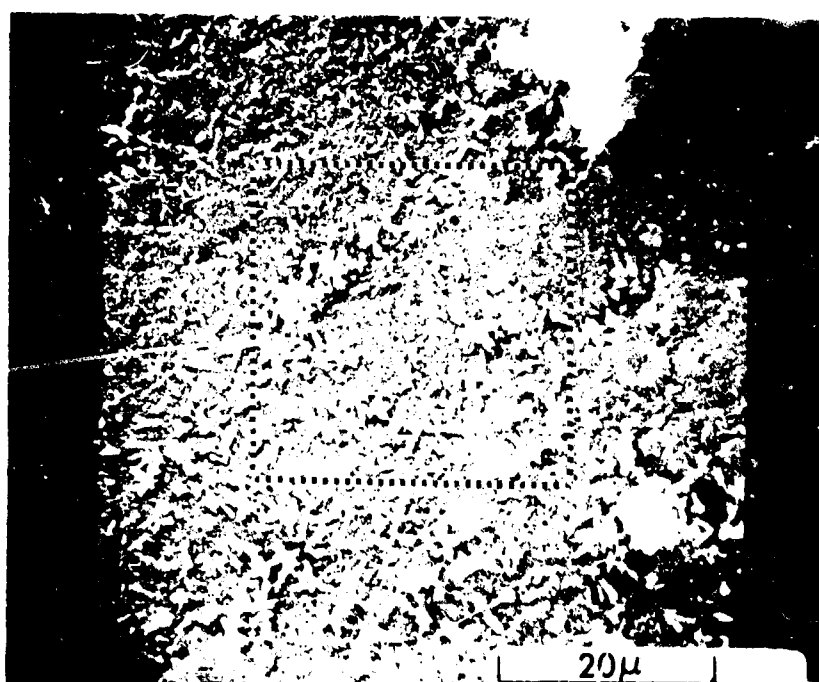
NOT REPRODUCIBLE



Figure 4.11 (continued from opposite page)... (b) A mosaic of micrographs showing approximately the same region as in (a) but with more detail. Notice the smoothness of the mortar with  $\text{CrO}_3$ .

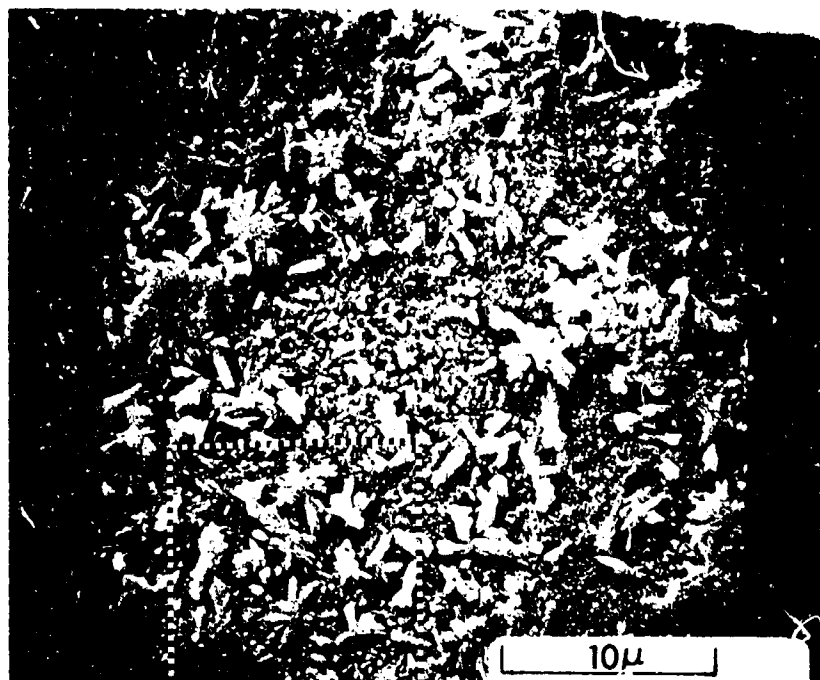


(a)



(b)

Figure 4.12. A sequence of higher magnification micrographs of the mortar surface with 10%  $\text{Ca}(\text{OH})_2$ . (a) This area is marked in Figure 4.11 (b) and can be identified by the loose particle in the upper portion of the micrograph. (b) A micrograph of an area marked in (a) which shows the microcrystalline texture of the surface.



(c)



(d)

Figure 4.12 (continued from opposite page)... (c) A higher magnification view of an area marked in (b) which shows the morphology of the crystals making up the surface. (d) A very high magnification micrograph of an area marked in (c) showing the dendritic nature of the crystals in the surface of the mortar.

increasing steps of magnification in Figure 4.12 (a b c d) in order to illustrate the surface texture of the mortar in contact with the reinforcing steel. The utility of the scanning electron microscope is evident in this sequence of micrographs where individual dendritic crystallites are visible in Figure 4.12 (d). It is probable that these are outer hydration products which nucleated and grew on the surface of the reinforcing steel to form the smooth interface between mortar and steel. This process can be imagined from the schematic illustrations in Figures 2.3 and 2.4. It is likely that the round flat crystals visible in Figure 4.12 (a b c) remained in contact with the steel and those in Figure 4.12 (d) shrunk back a few microns from the steel surface. The exact identity of the dendritic crystals visible in Figure 4.12 (d) cannot be made at this time since there is little experience on observations on this type of surface. There are several crystals visible in Figure 4.12 (c d) which have the sheaf of wheat morphology observed by Williamson (15) in transmission microscopy of tricalcium silicate ( $C_3S$ ) outer hydration products. It is also possible that this may be a carbonated layer on the free surface after the sample was cut open. In the latter case the morphology of the crystallites may be that of the original hydration products and retained as pseudomorphs in the carbonation layer; or it may be that of the carbonation products themselves.

#### 4.3. Conclusions and Recommendations

The galvanic cell between the plain steel and galvanized steel in ferro-cement is a problem which until this time appears to have been unknown. This cell has probably been active in most ferro-cement projects

with the resulting lower strength and durability. The inspection and licensing authorities should be aware of the galvanic cell problem in ferro-cement, and all projects constructed in the past should be viewed as weakened by the evolution of hydrogen at the ungalvanized reinforcing bar. One of the most effective inspection procedures would be to remove specimens from the structure and look at the interface between the mortar and the plain steel.

For all future ferro-cement construction, we recommend that  $\text{CrO}_3$  be added to the mixing water. Again the inspection and licensing authorities could require that  $\text{CrO}_3$  be used during construction and that its use be noted in the permanent records of the vessel or structure.

The testing and inspection of ferro-cement vessels is a relatively new field and we recognize that the discovery of the galvanic cell problem has complicated the inspection of existant vessels and structures. Further experiments should be performed to determine how the durability of these vessels or structures is affected by the poor bond between reinforcing steel and the mortar. A non-destructive test method should be developed to help the surveyor determine the extent of bubble formation in an existing panel of ferro-cement. As it stands at this time we can only recommend that test panels be cut from the vessel or structure and the interface inspected visually.

In the final analysis it is only in new construction that the galvanic cell problem can really be solved, and we believe that the addition of  $\text{CrO}_3$  is the best possible solution. We must go along with the quotation of A. L. Edge, "It's almost impossible to distinguish



between a good or poor quality ferro-cement hull after it has been finished," (16). A ferro-cement vessel or structure must be made correctly the first time because it is almost impossible to go back and fix it later.

# REFERENCES

1. S. P. Shah, "Ferro-Cement as a New Engineering Material, Univ. of Illinois at Chicago Circle Report No. 70-11, November 1970, presented at the Canadian Capital Section of American Concrete Institute, Ottawa, December 1970.
2. J. F. Collins and J. S. Claman, "Ferro-Cement for Marine Applications - An Engineering Evaluation," Department of Naval Architecture and Marine Engineering, Massachusetts Institute of Technology, Cambridge, Mass., March 1969.
3. G. W. Jackson and W. M. Sutherland, Concrete Boatbuilding, Its Technique and Its Future, John DeGraff Inc., N.W. (1969).
4. V. F. Bezukladov, K. K. Amel Vanovich, et al., "Ship Hulls Made of Reinforced Concrete," (Korpora Sudov Iz Amotsementa), transl. from Russian, Navships Trans. No. 1148, November 1968.
5. P. L. Nervi, "Ferro-Cement: Its Characteristics and Potentialities," L'Ingegnere (1951) or C.A.C.A. London Library, Translation 60 (1965).
6. R. B. Williamson, Solidification of Portland Cement, Rept. No. UCSESM 70-23, December 1970.
7. T. C. Powers, "Structure and Physical Properties of Hardened Portland Cement Paste," J. Am. Cer. Soc. 41 (1958) 1-6.
8. B. Bresler and I. Cornet, "Corrosion Protection of Steel Reinforcement in Concrete and Tentative Recommendations for Use of Galvanized Steel Reinforcement," Report to International Lead Zinc Research Organization, Inc., New York, N.Y., October 1969.
9. I. Cornet and B. Bresler, "Corrosion of Steel and Galvanized Steel in Concrete," Materials Protection, 5, 69-72, April 1966.
10. T. Ishikawa, I. Cornet, and B. Bresler, "Electrochemical Study of the Corrosion Behavior of Galvanized Steel in Concrete," Dept. of Civil Engineering, University of California Berkeley.
11. I. Cornet and B. Bresler, "Some Recent Developments in the Use of Galvanized Steel Reinforcement in Concrete," Internationale Verzinkertagung, Duesseldorf, December 6, 1970.
12. B. Bresler and I. Cornet, private communication.

13. K. A. Christensen, "The Impact Resistance of Laminated Steel Mesh Impregnated with Portland Cement Mortar (Ferro-Cement)," Graduate Research Project, Department of Civil Engineering, University of California, Berkeley, Spring 1970.
14. Charles Darwin Canby, "Ferro-Cement with Particular Reference to Marine Applications," Dept. of Naval Architecture and Marine Engineering, University of Michigan, October 1968.
15. R. B. Williamson, "Constitutional Supersaturation in Portland Cement Solidified by Hydration," J. Crystal Growth, 3, 4, (1968), 787-794.
16. J. R. Whitener, Ferro-Cement Boat Construction, Cornell Maritime Press, Inc., Cambridge, Md., 1971, p. 109.